Ontogeny of the skull of the blind snake *Amerotyphlops brongersmianus* (Serpentes: Typhlopidae) brings new insights on snake cranial evolution

MARIANA CHULIVER[1,2,*,], AGUSTÍN SCANFERLA[1] and CLAUDIA KOCH[2]

[1]*CONICET - Fundación de Historia Natural 'Félix de Azara', Hidalgo 775, Ciudad Autónoma de Buenos Aires C1405BCK, Argentina*
[2]*Leibniz Institute for the Analysis of Biodiversity Change, Adenauerallee 127, Bonn 53113, Germany*

Blind snakes represent the most basal group of extant snakes and include fossorial species with unusual skeletal traits. Despite their known phylogenetic position, little is known about their ontogeny and what it might reveal about the origin of their skull anatomy. Here we describe for the first time the ontogenetic transformations of the skull of a blind snake, the typhlopid *Amerotyphlops brongersmianus*, including embryos and postnatal individuals. Furthermore, we provide data on the size changes relative to skull growth of the main elements of the gnathic complex. We observed that the skull of this blind snake undergoes considerable morphological change during late ontogeny. Additionally, we detected delayed development of some traits (closure of the skull roof, opisthotic-exoccipital suture, ossification of the posterior trabeculae) simultaneously with clearly peramorphic traits (development of the crista circumfenestralis, growth of the pterygoid bar). Our analysis suggests that the unique skull anatomy of blind snakes displays plesiomorphic and highly autapomorphic features, as an outcome of heterochronic processes and miniaturization, and is shaped by functional constraints related to a highly specialized feeding mechanism under the selective pressures of a fossorial lifestyle.

ADDITIONAL KEYWORDS: development – fossorial snakes – growth – heterochrony – micro-CT – miniaturization – skull morphology.

INTRODUCTION

Blind snakes (Anomalepididae, Typhlopoidea and Leptotyphlopidae) represent the first extant branches in the evolutionary radiation of modern snakes (Miralles *et al.*, 2018; Burbrink *et al.*, 2020). They are fossorial forms with tubular bodies, smooth scales and a substantial reduction of eyes and head scalation (Vitt & Caldwell, 2009). They feed on social insects, such as ants, termites and their larvae (Cundall & Greene, 2000), using a singular intraoral prey transport mechanism called mandibular or maxillary raking (Kley, 2001). All elements of the gnathic complex (i.e. palatomaxillary bars, suspensorium and lower jaw) are involved during feeding, and toothed elements of the jaws (maxilla or dentary) are used to ratchet small prey into and through the mouth (Cundall & Greene, 2000;

Kley, 2001). Thus, the overall skull morphology of blind snakes is conditioned by their unique feeding system and the mechanical demands imposed by excavation (Cundall & Irish, 2008), deviating significantly from the general trends of squamates (Evans, 1955; Kley, 2006; Palci *et al.*, 2016; Da Silva *et al.*, 2018; Chretien *et al.*, 2019; Strong *et al.*, 2021).

The skull anatomy along with other particular traits constitute a set of characters called 'scolecoidy' (*sensu* Miralles *et al.*, 2018), an ecomorphotype shared by the three major clades of blind snakes. These clades represent successful groups of fossorial snakes, with more than 450 species currently recognized, and several new species (e.g. Koch *et al.*, 2015, 2016, 2019; Shea, 2015; Kraus, 2017; Dehling *et al.*, 2018) and genera (Martins *et al.*, 2019) described each year. They are distributed on all continents except Antarctica, with a long evolutionary history that probably pre-dates the Upper Cretaceous (Vidal *et al.*, 2010; Miralles *et al.*, 2018).

*Corresponding author. E-mail: marianachp@yahoo.com.ar

Ontogenetic studies are relevant to understand the processes responsible for morphological diversity and result in a powerful source of information about evolutionary patterns in the skeleton of squamates (e.g. Rieppel, 1992a, 1994; Maisano, 2001; Bhullar, 2012; Roscito & Rodriguez, 2012; Werneburg *et al.*, 2015; Da Silva *et al.*, 2018; Ollonen *et al.*, 2018; Khannoon *et al.*, 2020, among others). Regarding snakes, numerous studies have pointed to heterochronic processes as responsible to a large extent for morphological evolution of the group (Rieppel, 1988; Irish, 1989; Werneburg & Sánchez-Villagra, 2014), but they were solely based on adult specimens and no ontogenetic evidence was included to support their hypotheses. Additionally, the study of ontogenetic sequences may bring data on functionally-relevant transient structures (De Beer, 1940) that may be helpful to elucidate evolutionary aspects of different snake clades. Moreover, in spite of descriptions of skeletal ontogeny in snakes having increased and gaining relevance in recent years (Boback *et al.*, 2012; Polachowski & Werneburg, 2013; Khannoon & Evans, 2015; Palci *et al.*, 2016; Scanferla, 2016; Sheverdyukova, 2017; Al Mohammadi *et al.*, 2020), studies have been focused on the most widely known group of extant snakes (i.e. Alethinophidia).

To date, the cranial ontogeny of blind snakes remains largely unknown due to their secretive habits, which make them rarely encountered in the field, and scarce in museum collections (Koch *et al.*, 2019) with the exception of a few locally abundant species (McDiarmid *et al.*, 1999). Consequently, the study of ontogenetic series of these elusive snakes represents a challenge, and only a few observations regarding the postnatal ontogeny of the skull of certain species are available (Cundall & Irish, 2008; Palci *et al.*, 2016; Scanferla, 2016). However, there is a renewed interest in blind snake morphology, fuelled by new phylogenetic perspectives and the introduction of micro-CT technology to uncover the anatomy of these small-sized, often minute snakes (Bell *et al.*, 2021).

Amerotyphlops brongersmianus (Vanzolini, 1976) is a relatively large (snout-vent length = 300 mm on average) blind snake belonging to the family Typhlopidae. This oviparous species has recently been the focus of different studies, among which stands the detailed description of its adult osteology (Lira & Martins, 2021). Furthermore, it represents the first blind snake for which embryonic staging based on external morphology has been described (Sandoval *et al.*, 2020). In this line, the present study provides the first detailed description of the skull changes during embryonic and postnatal ontogeny of the blind snake *A. brongersmianus* through 3D reconstructions based on micro-CT data. This is presented within a comparative approach incorporating skulls of

embryos of alethinophidian species and lizards. In light of the relevance of developmental processes for understanding the evolution of blind snakes, this research represents a reliable source to test previous hypotheses of heterochronic processes occurring in this clade (e.g. Rieppel, 1988; Irish, 1989; Werneburg & Sánchez-Villagra, 2014; Da Silva *et al.*, 2018; Strong *et al.*, 2020).

MATERIAL AND METHODS

SPECIMENS

The ontogeny of the skull of *A. brongersmianus* was studied through embryos and postnatal specimens housed in the Herpetological Collection of Universidad Nacional del Nordeste (UNNEC), Corrientes, Argentina (Table 1). Three post-ovipositional embryos were selected based on the staging criteria of Sandoval *et al.* (2020), and four postnatal specimens were selected based on their snout-vent length (SVL). The smallest individual of the postnatal ontogenetic sequence was considered a hatchling due its SVL being lower than that of the hatchling reported by Sandoval *et al.* (2020). We recognized two stages between hatching and adult stage, designated as juvenile and subadult only for descriptive purposes since data on gonadal development of these specimens was not available.

Embryos of the anguimorph lizard *Lanthanotus borneensis* Steindachner, 1878 and the alethinophidian snake species *Liasis mackloti* Duméril & Bibron, 1844, *Candoia bibroni* (Duméril & Bibron, 1844) and *Naja oxiana* (Eichwald, 1831) were studied to make comparisons with structures of interest. Information about all specimens analysed is given in Table 1. Skulls of adult specimens of squamates available in the online repository MorphoSource (www.morphosource.org) were also examined for comparative purposes.

MICRO-CT

The head of each specimen was scanned on a Bruker SkyScan 1173 Micro-CT scanner at the Zoological Research Museum Koenig (ZFMK), Bonn, Germany. The scan parameters for each specimen are detailed in the Supporting Information (Table S1). Micro-CT data sets were reconstructed using N-Recon software (Bruker Micro-CT) and rendered in three dimensions through the aid of CTVox for Windows 64 v.2.6 (Bruker Micro-CT). We followed the terminology of Haluska & Alberch (1983), Cundall & Irish (2008) and Rieppel *et al.* (2009) for skull embryonic ontogeny and osteology.

MORPHOMETRIC ANALYSIS

In order to compare growth trajectories of the skeletal elements that constitute the gnathic complex (palatomaxillary bar, suspensorium and lower jaw), we measured selected bones and bony structures on 3D reconstructions of *A. brongersmianus* postnatal specimens (Table 2). The same measurements were taken on dry and cleared and stained skulls of postnatal ontogenetic sequences of representatives of the lizard outgroup Anguimorpha (*Ophiodes intermedius* Boulenger, 1894) and of the alethinophidian snake group (*Philodryas psammophidea* Günther, 1872). This alethinophidian snake species represents herein the macrostomous condition (i.e. ingestion of large prey with a large cross-sectional area in relation to the head dimensions of the snake; Cundall & Greene, 2000;

Table 1. Information about the specimens analysed. Abbreviations: UNNEC, Herpetological Collection of the Universidad Nacional del Nordeste, Corrientes (Argentina); ZFMK, Herpetological Collection of the Alexander Koenig Museum, Bonn (Germany)

Species	Specimen	SVL (mm)	Ontogenetic stage	Stage (author)
Amerotyphlops brongersmianus	UNNEC 10326	-	Posovipositional embryo	33 (Sandoval *et al.*, 2020)
Amerotyphlops brongersmianus	UNNEC 10356	-	Posovipositional embryo	34 (Sandoval *et al.*, 2020)
Amerotyphlops brongersmianus	UNNEC 11433	-	Posovipositional embryo	36 (Sandoval *et al.*, 2020)
Amerotyphlops brongersmianus	UNNEC 12783	84	Hatchling	-
Amerotyphlops brongersmianus	UNNEC 12831	120.5	Juvenile	-
Amerotyphlops brongersmianus	UNNEC 12796	190.6	Subadult	-
Amerotyphlops brongersmianus	UNNEC 12792	277.7	Adult	-
Lanthanotus borneensis	ZFMK 97200	58.7	Posovipositional embryo	13 (Werneburg *et al.*, 2015)
Liasis mackloti	ZFMK 41572	397	Posovipositional embryo	10 (Boughner *et al.*, 2007)
Candoia bibroni	ZFMK 41185	299	Posovipositional embryo	10 (Boughner *et al.*, 2007)
Naja oxiana	ZFMK 55961	216	Posovipositional embryo	8 (Khannoon & Evans, 2015) 10 (Jackson, 2002)

Table 2. Measurements of the bony elements and structures of the gnathic complex throughout postnatal ontogeny of the anguid lizard *Ophiodes intermedius*, the blind snake *Amerotyphlops brongersmianus* and the alethinophidian snake *Philodryas psammophidea*. All measurements are given in mm. Abbreviations: DL, dentary length; LjL, lower jaw length; PtL, pterygoid length; QL, quadrate length; SkL, skull length; SVL, snout-vent length; MCN, Museo de Ciencias Naturales de Salta, Salta (Argentina); UNNEC, Herpetological Collection of the Universidad Nacional del Nordeste, Corrientes (Argentina)

Species	Specimen	SkL	PtL	QL	DL	LjL	SVL
Ophiodes intermedius	MCN 4443	6.7	2.8	1.3	3.2	5.1	32.0
Ophiodes intermedius	MCN 4444	8.1	4.3	1.6	4.2	7.6	56.0
Ophiodes intermedius	MCN 4445	11.8	5.9	2.0	6.1	10.9	114.0
Ophiodes intermedius	MCN 4446	18.9	9.1	3.2	9.9	17.8	237.0
Amerotyphlops brongersmianus	UNNEC 12783	5.5	3.1	1.9	0.5	2.9	84.0
Amerotyphlops brongersmianus	UNNEC 12831	6.5	3.7	2.1	0.6	3.9	120.5
Amerotyphlops brongersmianus	UNNEC 12796	7.3	4.3	2.1	0.8	4.2	190.6
Amerotyphlops brongersmianus	UNNEC 12792	9.5	6.3	2.4	0.8	5.6	277.7
Philodryas psammophidea	MCN 190	11.4	7.3	2.3	6.2	11.6	213.0
Philodryas psammophidea	MCN 133	16.4	10.5	4.3	9.2	16.7	473.0
Philodryas psammophidea	MCN 187	18.5	12.9	5.7	10.4	20.7	631.0
Philodryas psammophidea	MCN 4447	22.4	18.5	7.8	13.3	27.9	1020.0

Scanferla, 2016). Measurements were taken with a dial calliper under a binocular microscope to the nearest 0.1 mm and are provided in Table 2. The skull length was measured from the anterior tip of the snout to the posterior end of the occipital condyle in dorsal view, while the lower jaws were measured from the anterior tip of the dentary to the posterior end of the retroarticular process in lateral view. Measurements of selected structures of the gnathic complex (pterygoid, quadrate, dentary and lower jaw) were simply quantified as a ratio of their length against skull length. Then, growth trajectories were evaluated by plotting this ratio against successive ontogenetic stages. Data analyses and visualization were conducted using R v.4.0.2 (R CoreTeam, 2020).

RESULTS

SNOUT COMPLEX

The snout region in *A. brongersmianus* is formed by nasals, a premaxilla, septomaxillae and vomers (Figs 1–3). In the earliest embryo available (Stage 33) all these elements are fully differentiated and ossified. During embryonic ontogeny, this region is slightly narrower than the braincase and goes through a marked shift upwards (Fig. 1A-C). The foramina typical of the snout of blind snakes are already present at Stage 33, distributed ventrally in the premaxilla and in the dorsal lamina of the nasals (Figs 2A, 3A). The premaxilla also exhibits a prominent anteromedial carina and three pointed processes: a single posteriorly oriented vomerine process and paired laterally oriented septomaxillary processes (Fig. 3). The ventral closure of the snout is completed by the septomaxillae and vomers, which jointly outline the fenestra vomeronasalis (Fig. 3). The borders of the fenestra are remodelled through ontogeny due to the growing ossification of the posterior border of the septomaxilla (Fig. 3A-F). As in all blind snakes, the prefrontals are incorporated into the snout region in *A. brongersmianus* and laterally limit the external narial opening (Fig. 1).

A fully differentiated egg tooth was observed in embryos of *A. brongersmianus* (Fig. 1A-C), which shows a contrasting morphology with respect to the egg tooth of other squamates examined (Fig. 4). It is attached at the base of the posterior process of the premaxilla, markedly displaced posteroventrally (Fig. 4B). The length of the egg tooth is almost half the height of the snout region in lateral view, it has a sigmoidal shape and projects downwards (Fig. 4B). In contrast, the egg teeth of the anguimorph lizard *La. borneensis* and alethinophidian snakes *Li. mackloti* and *Naja oxiana* are attached to the anterior edge

of the premaxilla (Fig. 4A, C, D). The egg tooth of these species is short and markedly curved forward, thus it protrudes from the tip of the snout (Fig. 4A, C, D). In terms of morphology, the egg tooth of *A. brongersmianus* is conical with pointed tip, and has a rounded central cavity that narrows proximodistally (Fig. 4B). In this regard, the egg teeth of the lizard *La. borneensis* and both alethinophidian snake embryos are compressed anteroposteriorly and their width slightly decreases distally. In *La. borneensis*, the egg tooth's distal third narrows, ending in a rounded tip and its central cavity is circular in cross section (Fig. 4A), whereas the egg teeth of *Li. mackloti* and *N. oxiana* have a truncated end and their central cavity is a horizontal ellipse (Fig. 4C, D).

BRAINCASE ROOF

Paired frontals, a single parietal and paired supraoccipitals constitute the braincase roof of *A. brongersmianus*. Prootics, otooccipitals and stapes form the posterolateral (otic) region of the braincase, and the parabasisphenoid and basioccipital form the braincase floor (i.e. basicranium). At Stage 33, the supraoccipital, prootic, otooccipital and basioccipital are well ossified, but all these elements remain separated from one another by narrow unossified zones (Figs 1A, 2A, 3A).

The lateral descending flange of the frontal bone is the first portion to ossify during embryonic development, then the ossification progresses dorsally towards the dorsal lamina. In the late embryo (Stage 36), the dorsal lamina is well developed anteriorly but its posteromedial region is still unossified (Fig. 2C). The dorsal lamina of the frontal grows forwards and backwards during postnatal ontogeny. Therefore, an expansion of its anterior border between the nasals is observed and the frontoparietal suture is shifted posteriorly (Fig. 2D-F). Furthermore, there is a lateromedial compression of the frontals from juvenile to adult stages and a posterior process abutting against the postorbital process of the parietal develops at the adult stage (Fig. 2F).

The parietal is the only component of the braincase starting its ossification as a paired element and subsequently merging as an azygous bone. The ossification of the parietal begins in the descensus parietalis, and as the development progresses, it spreads dorsally towards the midline, constituting paired dorsal laminae which ultimately fuse. A wide gap still separates both dorsal laminae in the late embryo (Stage 36; Fig. 2C), but at the hatching stage only a small suture remains posteriorly in the midline (Fig. 2D). Furthermore, the ossification of the dorsal laminae of the parietals is notably delayed when compared to the ossification of the frontals at all
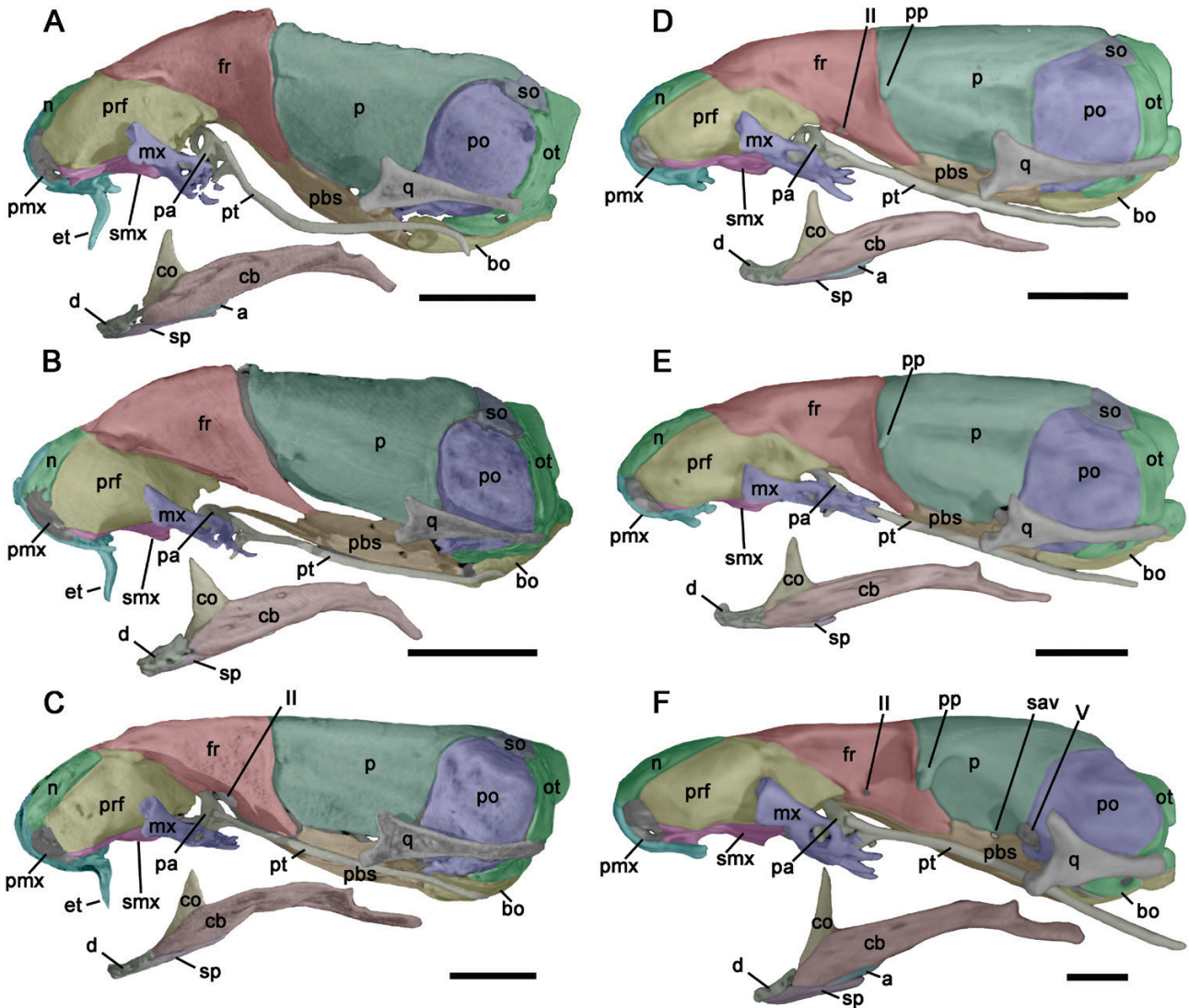
Figure 1. Lateral view of the skull of *Amerotyphlops brongersmianus* throughout embryonic and postnatal ontogeny: A, embryo at Stage 33; B, embryo at Stage 34; C, embryo at Stage 36; D, hatchling; E, juvenile; F, adult. Abbreviations: a, angular; bo, basioccipital; cb, compound bone; co, coronoid; d, dentary; et, egg tooth; fr, frontal; mx, maxilla; n, nasal; ot, otooccipital; p, parietal; pa, palatine; pbs, parabasisphenoid; pmx, premaxilla; po, prootic; pp, postorbital process; prf, prefrontal; pt, pterygoid; q, quadrate; smx, septomaxilla; so, supraoccipital; sp, splenial; II, foramen for the optic nerve; V, foramen for both rami of the trigeminal nerve. Scale bars equal to 1 mm.

embryonic stages (Fig. 2A-C). As with frontals, there is a remarkable dorsal remodelling of the parietal during postnatal ontogeny. It changes from rounded at the hatchling stage to a compressed configuration in adulthood (Fig. 2D-F). The anterolateral crest of the dorsal laminae projecting laterally in the contact zone with the frontals, and the posterolateral corner partially covering the suture between the prootic and supraoccipital (named the supratemporal process) are constituted late during postnatal ontogeny (Fig. 2E-F). The descensus parietalis approaches the parabasisphenoid along its lateral edge, although there

is a persistent gap along almost the entire ontogenetic sequence (Fig. 3A-E).

There is a mid-dorsal gap between both supraoccipitals during embryonic ontogeny but they approach each other at the midline at the hatching stage (Fig. 2A-D). The supraoccipital also undergoes shape changes from hatching stages to adulthood. Its anterior margin changes from rounded to straight in the dorsal view, while its lateral margin narrows. Both changes are tightly linked to shape change of the parietal described above, mostly related to growth of the supratemporal process.
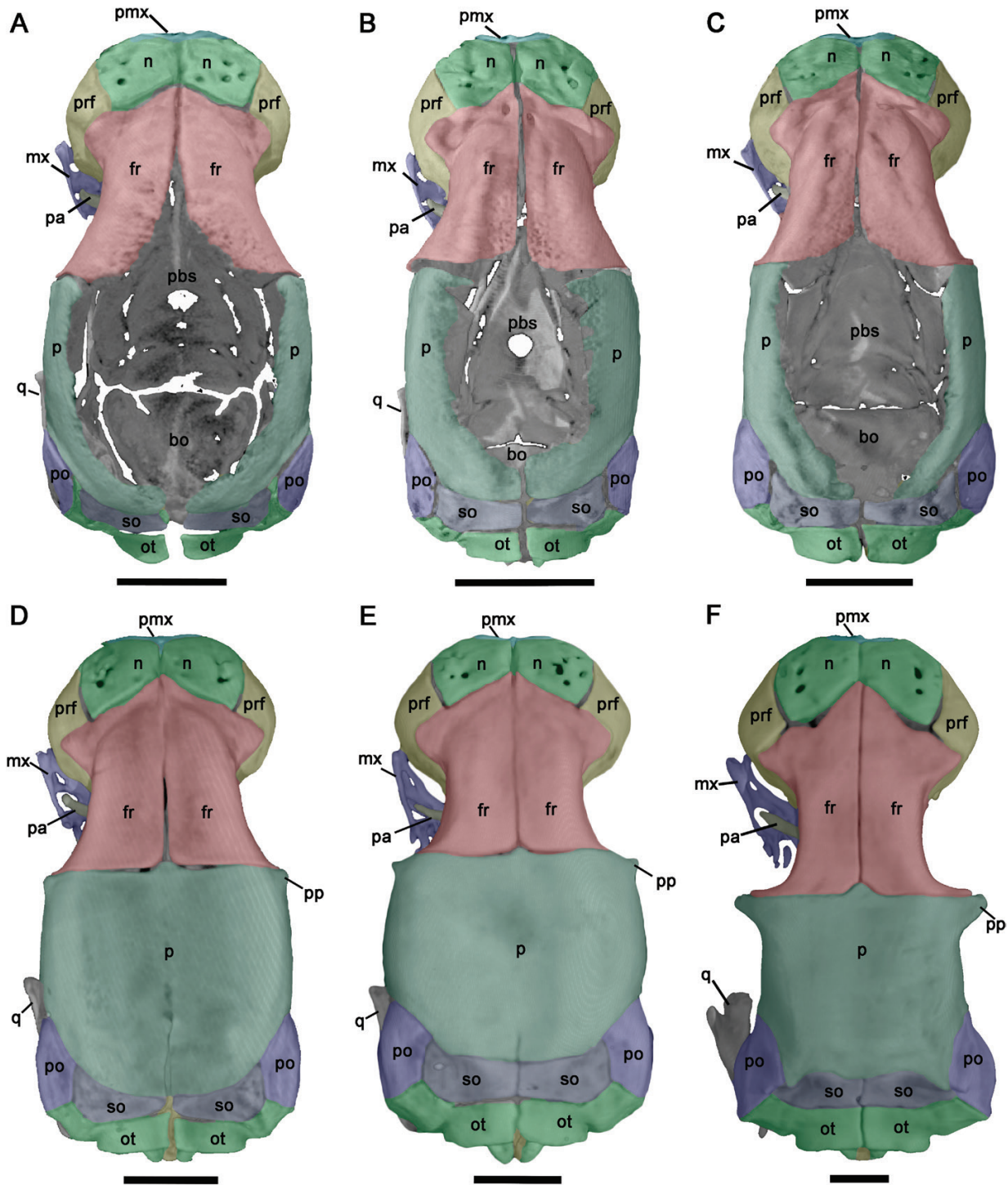
Figure 2. Dorsal view of the skull of *Amerotyphlops brongersmianus* throughout embryonic and postnatal ontogeny: A, embryo at Stage 33; B, embryo at Stage 34; C, embryo at Stage 36; D, hatchling; E, juvenile; F, adult. Abbreviations: bo, basioccipital; fr, frontal; mx, maxilla; n, nasal; ot, otooccipital; p, parietal; pa, palatine; pbs; parabasisphenoid; pmx; premaxilla; po, prootic; pp, postorbital process; prf, prefrontal; q, quadrate; so, supraoccipital. Scale bars equal to 1 mm.
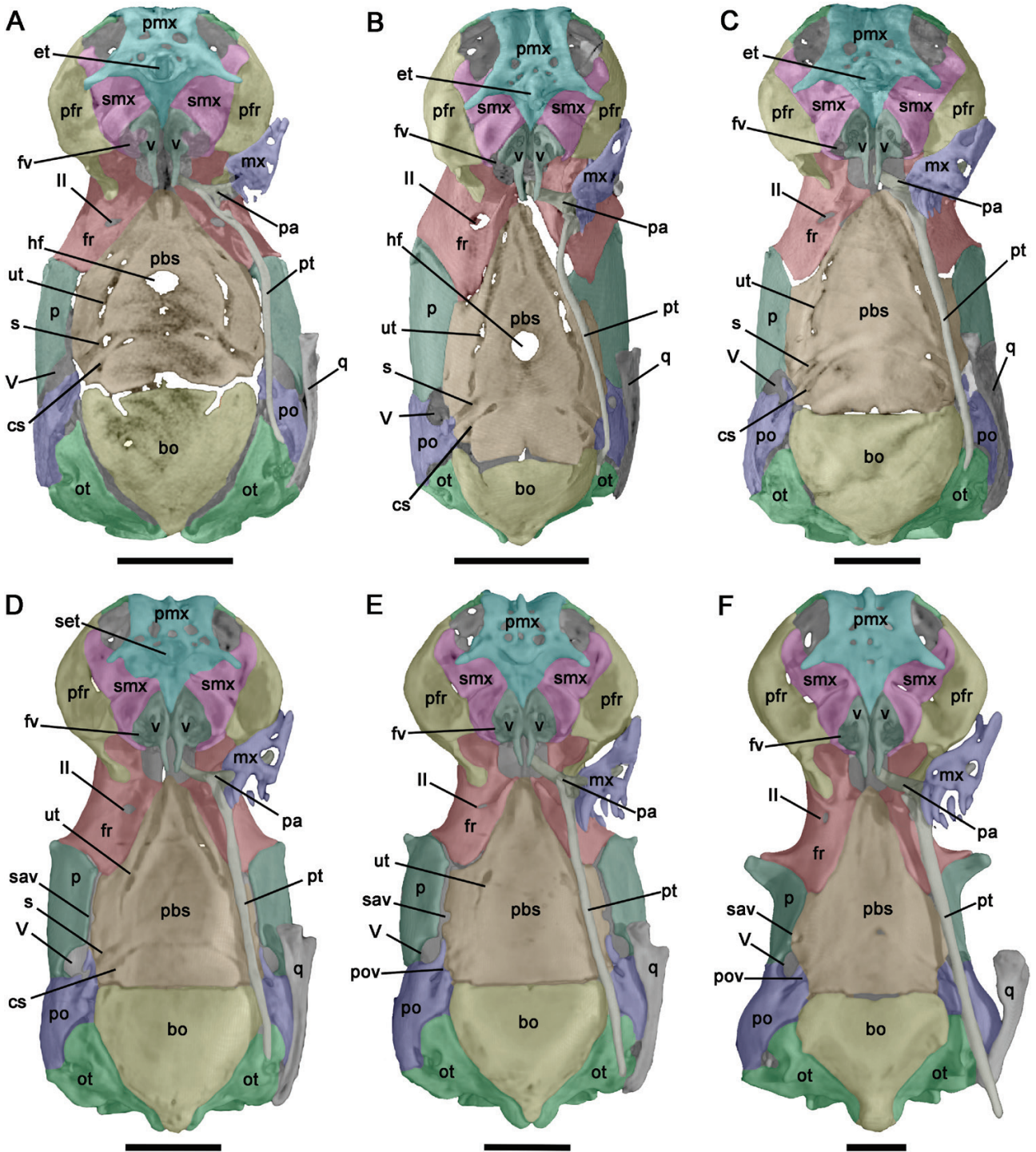
Figure 3. Ventral view of the skull of *Amerotyphlops brongersmianus* throughout embryonic and postnatal ontogeny. Lower jaw as well as the maxilla, palatine and pterygoid on the left side were digitally removed: A, embryo at Stage 33; B, embryo at Stage 34; C, embryo at Stage 36; D, hatchling; E, juvenile; F, adult. Abbreviations: bo, basioccipital; cs, crista sellaris; et, egg tooth; fr, frontal; fv, fenestra vomeronasalis; hf, hypophysial fenestra; mx, maxilla; ot, otooccipital; p, parietal; pa, palatine; pbs, parabasisphenoid; pmx, premaxilla; po, prootic; pov, posterior opening of the Vidian canal; pfr, prefrontal; pt, pterygoid; q, quadrate; s, sulcus of the embryonic parabasisphenoid; sav, secondary anterior opening of the Vidian canal; set, scar of the egg tooth; smx, septomaxilla; ut, unossified trabecula; II, foramen for the optic nerve; V, foramen for maxillary and mandibular rami of the trigeminal nerve. Scale bars equal to 1 mm.
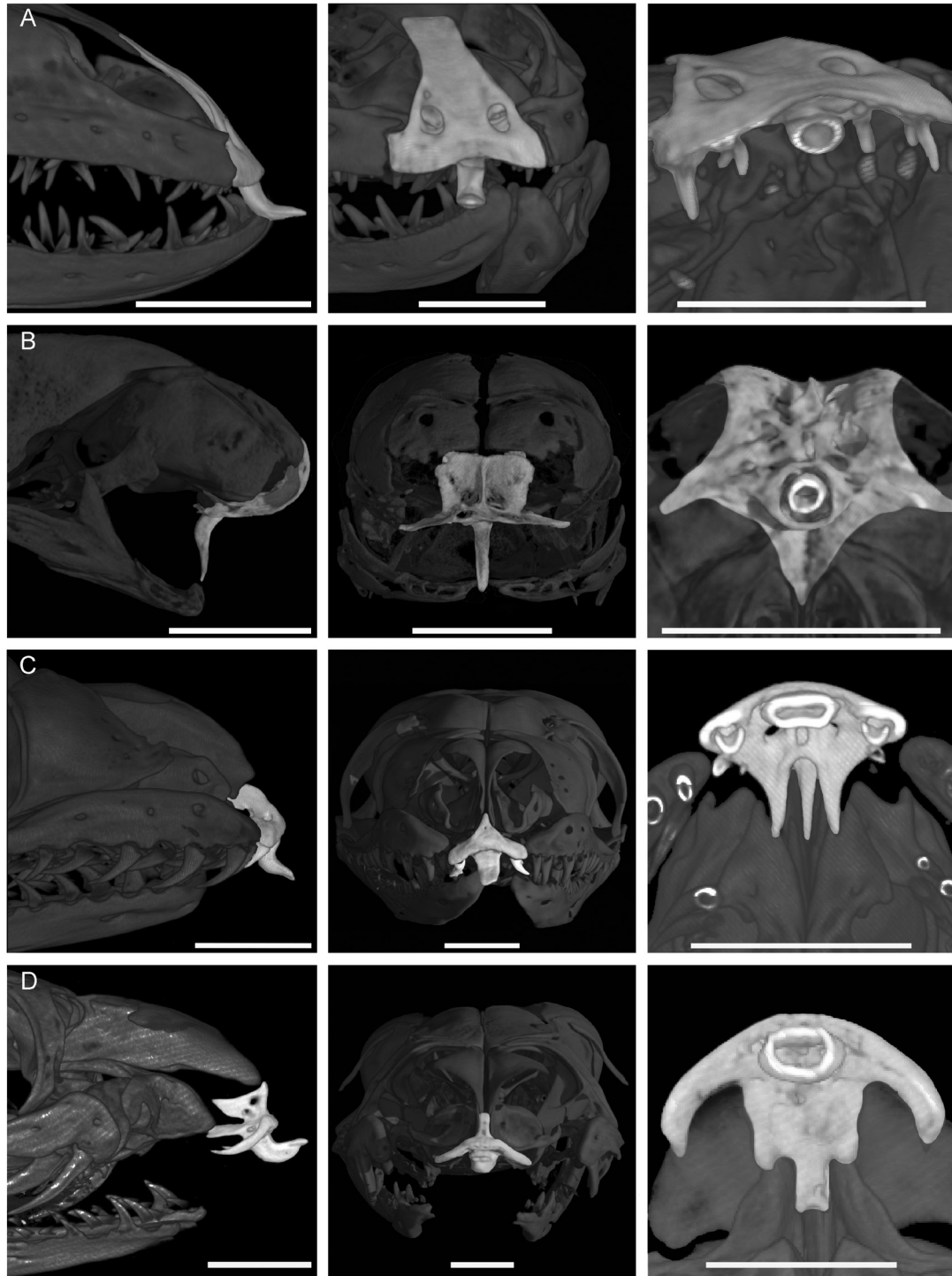
Figure 4. Lateral (left), anterior (centre) and ventral (right) views of the egg tooth of squamate embryos at equivalent pre-hatching stages: A, *Lanthanotus borneensis*; B, *Amerotyphlops brongersmianus*; C, *Liasis mackloti*; D, *Naja oxiana*. The premaxilla is highlighted in light grey. The ventral view is a horizontal cutaway showing the section of the egg tooth near its base. Scale bars equal to 1 mm.

OTIC REGION

The bony elements belonging to the otic region are differentiated and in an advanced stage of ossification at Stage 33 (Figs 1–3). The prootic occupies the posterolateral surface of the skull, and it expands in an anteroposterior direction during postnatal ontogeny
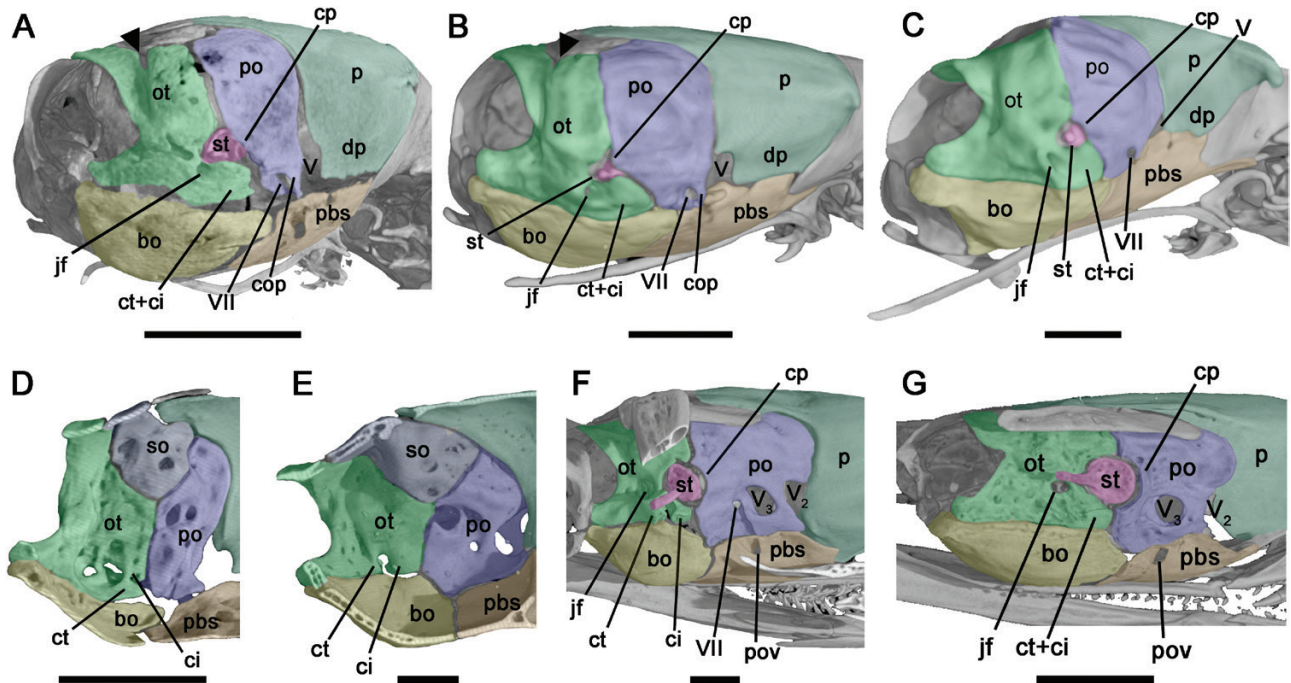
Figure 5. A-C, posterolateral views of the otic region of *Amerotyphlops brongersmianus* throughout ontogeny: A, embryo at Stage 33; B, hatchling; C, adult. Black arrowheads indicate the suture between the exoccipital and opisthotic. D, endocranial view of the otic region in an embryo of *A. brongersmianus* at Stage 34 showing the crista interfenestralis concealing the crista tuberalis. E-F, endocranial and lateral views of the otic region of the embryo of *Candoia bibroni* showing the type 3 configuration of the crista circumfenestralis. G, lateral view of the otic region of the embryo of *Naja oxiana* showing the type 4 configuration of the crista circumfenestralis. Abbreviations: bo, basioccipital; ci, crista interfenestralis; cop, commissura praefacialis; cp, crista prootica; ct, crista tuberalis; ct+ci, fused crista tuberalis and crista interfenestralis; dp, descensus parietalis; jf, jugular foramen; ot, otooccipital; p, parietal; pbs, parabasisphenoid; po, prootic; pov, posterior opening of the Vidian canal; so, supraoccipital; st, stapes; V, foramen for the maxillary and mandibular rami of the trigeminal nerve; V_2, foramen for the maxillary ramus of the trigeminal nerve; V_3, foramen for the mandibular ramus of the trigeminal nerve; VII, foramen for the facial nerve. Scale bars equal to 1 mm.

(Fig. 1D-F). The sole trigeminal foramen is located in the contact zone of the prootic, the descensus parietalis and the parabasisphenoid (Fig. 3). The contribution of the parabasisphenoid to the margins of this foramen may vary, since the prootic seems to exclude the parabasisphenoid at some stages during postnatal ontogeny (Fig. 3D, E).

The two elements that constitute the otooccipital (i.e. opisthotic and exoccipital) are distinguishable in the embryo at Stage 33. The dorsomedial and ventral parts of the otooccipital correspond to the exoccipital contribution, while the anterolateral portion bears on the opisthotic contribution (Fig. 5A). The suture between the exoccipital and opisthotic is still present in the late embryo (Stage 36) and remains at the hatching stage as a small gap restricted to the dorsal region of the bone (Fig. 5B). In the examined embryo of the anguimorph lizard, *La. borneensis*, both elements are unfused, whereas in the embryos of the alethinophidian snakes (*Candoia* Gray, 1842, *Liasis* Gray, 1842 and *Naja* Laurenti, 1768), the fusion

between elements is advanced and only a small suture in the dorsal region of the otooccipital is observed.

As in most blind snakes, in the adult stage of *A. brongersmianus* the stapedial footplate is almost concealed by the crista circumfenestralis and only the short stapedial shaft emerges from the juxtastapedial recess (Fig. 5C). Additionally, the crista tuberalis is expanded and has incorporated the crista interfenestralis. This morphology corresponds with the type 4 configuration of the crista circumfenestralis described by Palci & Caldwell (2014) for adult blind snakes and most colubroids. The available ontogenetic sequence shows a progressive growth of the crista prootica and crista tuberalis until reaching adult configuration (Fig. 5A-C). Embryos of *A. brongersmianus* show an extreme anterodorsal development of the crista tuberalis, which in turn, laterally conceals the small crista interfenestralis. Then, the crista interfenestralis is not visible as a discrete element laterally during embryonic development (Fig. 5A). Instead, the

contribution of both cristae (crista tuberalis and crista interfenestralis) can be seen medially in the otic region of *A. brongersmianus* embryos (Fig. 5D). The alethinophidian *C. bibroni* shows a contrasting morphology of the crista circumfenestralis (Fig. 5E, F), bearing a type 3 configuration (*sensu* Palci & Caldwell, 2014). The embryo of the colubroid *Naja oxiana* also bears the type 4 configuration of the crista circumfenestralis (Fig. 5G), although unlike *A. brongersmianus*, the crista interfenestralis seems to reach the lateral wall of the skull, and then fuse with the crista tuberalis. Hence, despite the type 4 configuration being present in adults of both species, their development follows different pathways.

<div align="center">BASICRANIUM</div>

The compound parabasisphenoid is in advanced stage of ossification in the examined Stage 33 of *A. brongersmianus* (Fig. 3A), thus it is not possible to discern the extent of the contribution of each former element—the membranous parasphenoid and the chondral basisphenoid—to adult bone. The subcircular hypophysial fenestra, located in the centre of the parabasisphenoid, is well developed in early embryos (Stages 33–34; Fig. 3A, B), but closed in the late embryo (Stage 36) and the hatching stage (Fig. 3C, D). Likewise, a small remnant of the basicranial fenestra is present between the posterior border of the parabasisphenoid and the anterior border of the basioccipital at Stage 36, but it is fully closed at the hatching stage (Fig. 3C, D). The posterior tip of the basioccipital, jointly with ventromedial projections of the otoccipital, form the occipital condyle in the adult stage (Figs 3F, 5C).

The cartilaginous regions corresponding to the trabeculae cranii and the crista sellaris (derived from the acrochordal cartilages) are seen as zones in light grey or even as empty spaces in Micro-CT images of embryos and hatchlings of *A. brongersmianus* (Fig. 3A-D), thus outlining part of the chondrocranium. These cartilages establish a triangular structure that acts as a scaffold from where most of the parabasisphenoid ossifies (Fig. 6A, B). In *A. brongersmianus*, the trabeculae diverge immediately posterior to the trabecula communis, in contrast to alethinophidians where the trabeculae run almost parallel most of their length (Fig. 6A-C). Furthermore, in adult alethinophidians there is a ridge named the crista trabecularis in the transition zone between cartilaginous and ossified trabecula in the parabasisphenoid, lateral to the base of the parasphenoidal rostrum. This structure is not observed in the adult of *A. brongersmianus* (Fig. 6B). Interestingly, the posterior portion of the trabeculae remain cartilaginous (at least their centre) until the juvenile stage in *A. brongersmianus* (Fig. 6D), while in alethinophidians they are ossified at embryonic stages.

There is an important bone outgrowth in the posterolateral region of the embryonic parabasisphenoid, probably originated as perichondral ossification from the trabecula, the crista sellaris, the basal plate or a combination of them (Fig. 6A). In this region the Vidian canal is formed, a complex structure for the passage of nerves and vessels. In ventral view, embryos show a sulcus and a foramen (i.e. posterior Vidian opening) in the posterolateral region of the parabasisphenoid (Fig. 3A, C). This sulcus is gradually floored during late embryonic and early postnatal stages, thus defining a duct named the closed Vidian canal (Figs 3C-D, 6A, B). The medial opening of this duct forms the dorsolateral margin of the cerebral carotid foramen as in alethinophidians (Fig. 6B, C, E-F, H-I). The lateral opening of the duct is the primary anterior opening of the Vidian canal and leads to an open groove—the Vidian groove—on the dorsal surface of the parabasisphenoid (Fig. 6B, F). The Vidian groove runs forwards and ends in an opening near the lateral rim of the parabasisphenoid, named the secondary anterior opening of the Vidian canal (Fig. 6B, F). This opening can be fully incorporated to the parabasisphenoid or be formed by this element and the parietal, showing asymmetrical variation in the same individual (Fig. 6F-G). Late embryos of *Candoia* (Fig. 6H) and *Liasis* show a similar intracranial morphology of the Vidian canal, bearing a short passage through the parabasisphenoid (i.e. closed Vidian canal) and a primary anterior opening at the level of the cerebral carotid foramen (Fig. 6H).

<div align="center">PALATOMAXILLARY BAR</div>

The palatomaxillary bar is formed by the maxilla, the palatine and the pterygoid rod (Figs 1, 3). The wide posterior half of the maxilla bears four tooth positions from embryonic to subadult stages, and the final five tooth count is reached in adult specimens. The pterygoid is a rod-like element, anteriorly bifurcated, that runs along the ventrolateral border of the skull (Fig. 3F). During embryonic development, the pterygoid changes from lateroventrally curved to straight, and it never surpasses the posterior limit of the prootic in lateral view (Figs 1A-C, 3A-C). In contrast, during postnatal ontogeny it doubles its length until reaching adult proportions, its posterior tip being projected beyond the occipital condyle (Fig. 1D-F).

<div align="center">SUSPENSORIUM AND LOWER JAW</div>

The quadrates suspend the lower jaw from the skull and have three main processes: an anterodorsal cephalic process, an anteroventral mandibular process
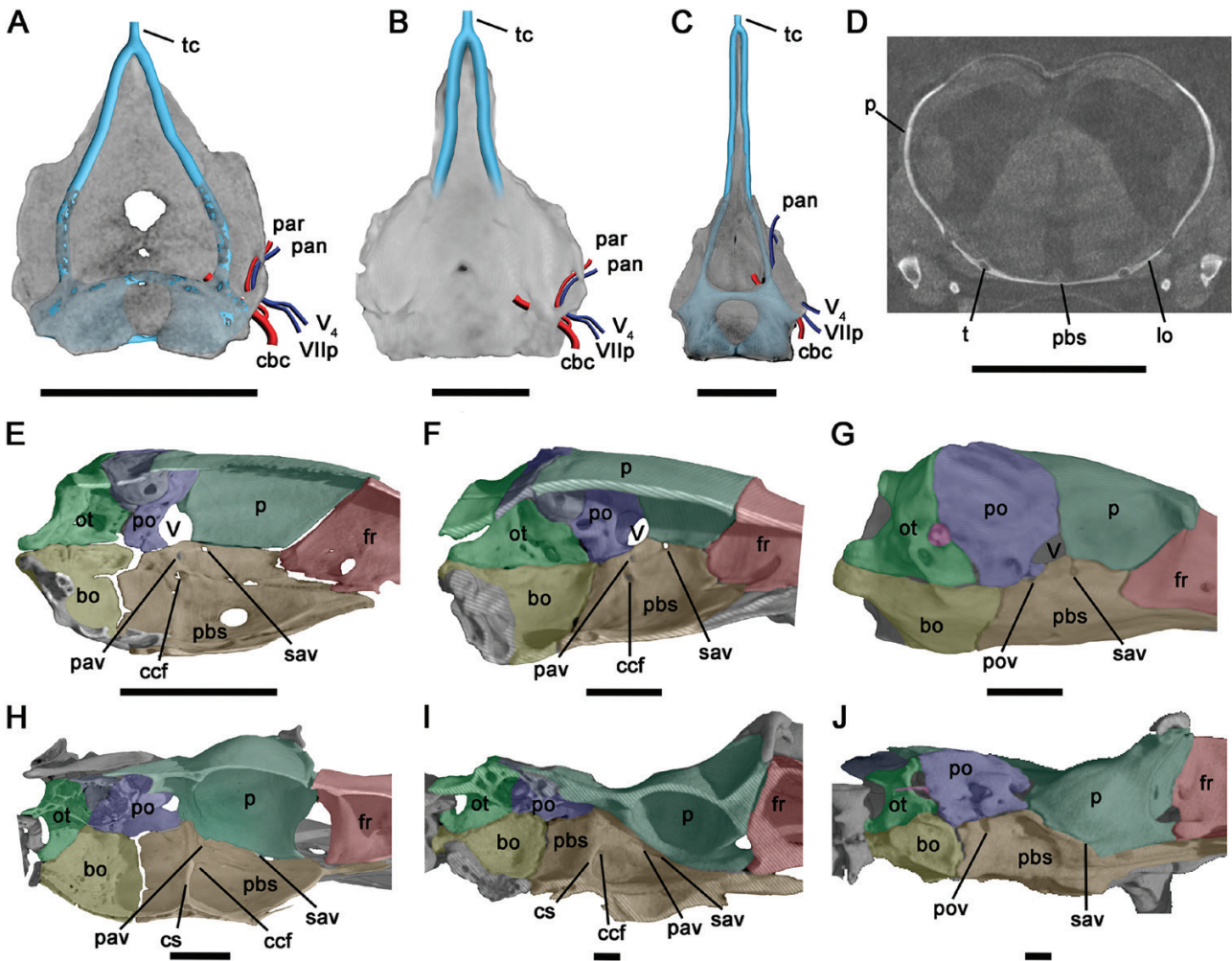
Figure 6. A-B, internal (endocranial) view of the parabasisphenoid bone in *Amerotyphlops brongersmianus* throughout ontogeny showing the conformation of the Vidian canal: A, embryo at Stage 33; B, adult. C, endocranial view of the parabasisphenoid bone of the embryo of *Liasis mackloti*. D, frontal cutaway posterior to the hypophysial fenestra of embryo of *A. brongersmianus* at Stage 33 showing the cartilaginous nuclei of the trabeculae cranii. E-F, internal views of a sagittal cutaway of the skull of *A. brongersmianus* throughout ontogeny showing different endocranial apertures of the Vidian canal and presence of the lateral wing of the parabasisphenoid: E, embryo at Stage 33; F, adult. G, lateroventral view of the adult skull of *A. brongersmianus* showing external apertures of the Vidian canal. H-I, internal views of a sagittal cutaway of the skull of *Candoia bibroni* throughout ontogeny showing different endocranial apertures of the Vidian canal and the lateral wing of the parabasisphenoid: H, embryo; I, adult. J, lateroventral view of the adult skull of *C. bibroni* showing external apertures of the Vidian canal. Abbreviations: bo, basioccipital; cbc, cerebral carotid artery; ccf, cerebral carotid foramen; fr, frontal; lo, lateral ossification of the posterior trabecula; ot, otooccipital; p, parietal; pan, palatine nerve; par, palatine artery; pav, primary anterior opening of the Vidian canal; pbs; parabasisphenoid; po; prootic; pov, posterior opening of the Vidian canal; sav, secondary anterior opening of the Vidian canal; t, trabecula cranii; tc, trabecula communis; V, foramen for the maxillary and mandibular rami of the trigeminal nerve; V_4, cid nerve; VII_p, palatine ramus of the facial nerve. Scale bars equal to 1 mm.

and a posterior suprastapedial process (Fig. 1F). During embryonic development, the anterior region of the bone surpasses the anterior border of the prootic, reaching the posterior half of the parietal (Fig. 1A-C). However, in the adult stage the quadrate does not surpass the prootic anteriorly (Fig. 1F; see below for further explanation). In addition, the quadrate

bone does not experience rotation along embryonic development, but it progressively opens laterally during postnatal ontogeny (Fig. 3E, F) as was also described by Palci *et al.* (2016) for the typhlopid *Anilios bicolor* (Peters, 1858).

The lower jaw in adult specimens of *A. brongersmianus* is formed by the dentary, the splenial, the
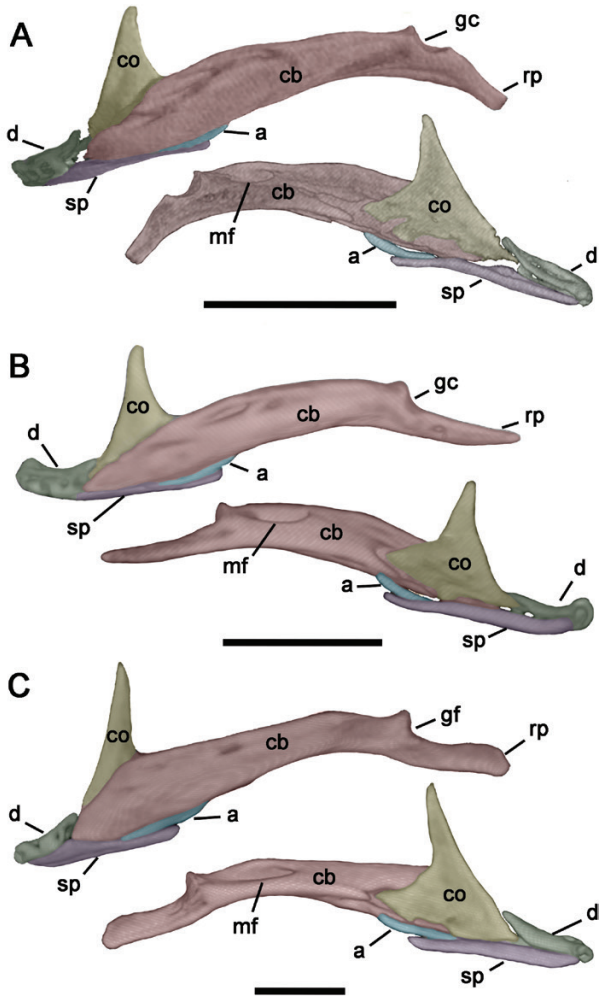
Figure 7. Lateral and medial views of the lower jaw of *Amerotyphlops brongersmianus* throughout ontogeny: A, embryo at Stage 33; B, hatchling; C, adult. Abbreviations: a, angular; co, coronoid; cb, compound bone; d, dentary; gc, glenoid cavity; mf, mandibular fossa; rp, retroarticular process; sp, splenial. Scale bars equal to 1 mm.

angular, the coronoid and the compound bone (Fig. 7C). The embryo at Stage 33 exhibits these elements as well differentiated and in an advanced stage of ossification (Fig. 7A). There are no traces of tooth sockets nor teeth along the lower jaw of the embryo at Stage 33 (Fig. 7A). The Meckelian canal is open medially between the dentary and splenial, and in the anterior region of the compound bone (Fig. 7A). The ossification of these bones increases during embryonic ontogeny closing the canal medially (Fig. 7B). Additionally, in the embryo at Stage 33, the anterior portion of the compound bone exhibits a longitudinal ventral gap which separates a major ossification spreading on the dorsolateral face of the mandible from a ventromedial ossification. They may correspond to the prearticular and the surangular contributions to the compound bone, respectively.

GROWTH OF THE GNATHIC COMPLEX

The size changes of the bones of the gnathic complex—relative to linear skull growth—in *A. brongersmianus* involve an overall allometric growth, except for the dentary (Figs 7, 8). Notably, the pterygoid experiences a positive allometric growth during postnatal ontogeny as is also the case for the alethinophidian snake *Philodryas psammophidea* (Fig. 8). The relative size of the quadrate decreases with increasing ontogenetic stage in *A. brongersmianus* and in the anguimorph lizard *Ophiodes intermedius*, opposite to what occurs in macrostomous alethinophidian snakes, as exemplified herein by *P. psammophidea* (Fig. 8). This negative allometric growth of the quadrate, along with its postnatal lateral aperture, lead to the postnatal change of position of the anterior region of the quadrate with respect to the braincase mentioned above.

Growth of the lower jaw shows similar trends across examined species, with a relative increase of the size occurring throughout ontogeny although less markedly pronounced in *A. brongersmianus* (Fig. 8). The relative growth of the dentary of *A. brongersmianus*, graphically represented as a flat line almost parallel to the *x*-axis, is noteworthy (Fig. 8). This bone grows isometrically along the ontogeny, suggesting that its small size in adult forms is the result of proportions established during early embryonic stages (Fig. 7A). Therefore, the compound bone is likely the main element contributing to the overall length of the lower jaw in *A. brongersmianus*.

DISCUSSION

The study of the skull ontogeny of *A. brongersmianus* allowed the description of transient structures (the egg tooth), the identification of some traits (closure of the skull roof, fusion of elements of otoccipital bone, ossification of the trabeculae cranii) for which development is delayed compared to alethinophidian snakes, and of phylogenetically relevant characters (the lateral wings of the parabasisphenoid) for blind snakes. Furthermore, the compiled information permitted us to link particular characteristics of the adult skulls with heterochronic processes, and relate them to the evolutionary processes that shaped cranial anatomy of this group (miniaturization and fossoriality).

EGG TOOTH

The presence of one egg tooth was described as the predominant condition in Squamata, and was employed along with molecular data to define the large clade Unidentata (Vidal & Hedges, 2005, 2009). In spite of the phylogenetic relevance of this character,
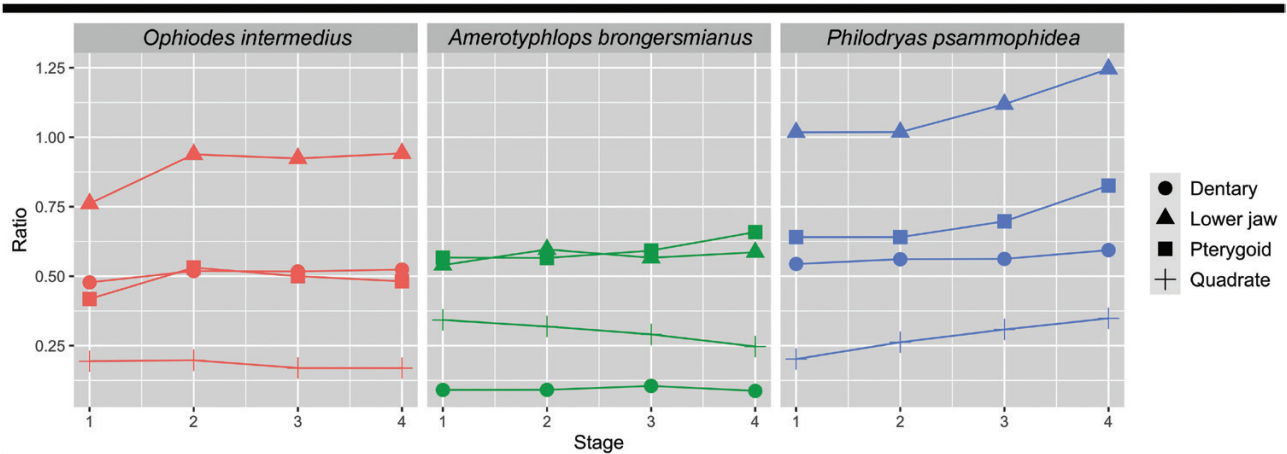
Figure 8. Ratio between the length the bones of the gnathic complex and linear skull length plotted against postnatal ontogenetic stages of the anguimorph lizard *Ophiodes intermedius*, the blind snake *Amerotyphlops brongersmianus* and the alethinophidian snake *Philodryas psammophidea*. The successive postnatal ontogenetic stages were ordered according to SVL and named from 1 to 4 corresponding to hatching, juvenile, subadult and adult stages respectively.

knowledge about early stages of its development and differentiation is scarce (Hermyt *et al.*, 2017, 2020a; Fons *et al.*, 2019). Previous studies reported the egg tooth rudiments in the Unidentata as either paired or unpaired, and described two different developmental pathways for paired rudiments according to the squamate group (Anan'eva & Orlov, 2013; Hermyt *et al.*, 2020b). In anguimorph lizards and alethinophidian snakes both rudiments merge to form a single egg tooth (Smith *et al.*, 1952; Anan'eva & Orlov, 2013; Fons *et al.*, 2019). This particular developmental pathway results in an egg tooth with a horizontally elongated base (Fons *et al.*, 2019). If the shape of the base of the egg tooth is considered a predictor of its developmental origin, then the subcircular base of the egg tooth of *A. brongersmianus* may indicate no early convergence between rudiments, and therefore may involve a developmental pathway different from that of alethinophidians. However, histological or molecular tools to study early embryos are necessary to accurately test this hypothesis.

The egg tooth of *A. brongersmianus* described herein represents the first report of this structure in a blind snake. It remains distinctive to all egg teeth described for squamates up to now due to its unique position and remarkable length and orientation (De Beer, 1949; Smith *et al.*, 1952; Trauth, 1988; Underwood & Lee, 2000; Anan'eva & Orlov, 2013; Hermyt *et al.*, 2017, 2020a, b; Fons *et al.*, 2019). We consider that the main features of the egg tooth of *A. brongersmianus* respond to a functional compromise with traits of the elements of the gnathic complex and the resulting particular morphology of the mouth. The snout region of blind snakes appears to have rotated ventrally (Cundall & Irish, 2008), shifting the premaxilla over the ventral surface of this region (Fig. 3). This shift may also entail a posterior displacement of the dentigerous zone of this bone and the consequent position of the egg tooth into the mouth cavity. In addition, as a result of the strongly reduced dentary, the lower jaw of typhlopids does not contact the tip of the snout when the mouth is closed (Rieppel *et al.*, 2009). Accordingly, length and orientation of the egg tooth could be related to the ventrally located mouth opening.

Regarding its function, Smith *et al.* (1952) described the egg tooth of some viperids—*Sistrurus catenatus* (Rafinesque, 1818), *Vipera aspis* (Linnaeus, 1758) and *Vipera berus* (Linnaeus, 1758)—as pointing downwards, and suggested this orientation corresponds to a loss of function due to the viviparous condition of the species. However, as we noted herein, the egg tooth of *A. brongersmianus* in spite of being displaced into the mouth cavity and directed downwards, may still perform its function due to the ventrally directed mouth opening. Therefore, the egg tooth of *A. brongersmianus* may correspond to a new category of Fioroni's (1962) classification, where three types of egg teeth were described for snakes according to characters of their morphology and function.

BRAINCASE ROOF

Several authors recorded skull ossification in alethinophidian snake species and reported the onset of ossification of the parietals in the ventrolateral region of the skull, progressing dorsally and reaching the midline during embryonic development (Haluska & Alberch, 1983; Rieppel & Zaher, 2001; Boughner *et al.*, 2007; Boback *et al.*, 2012; Polachowski & Werneburg, 2013; Sheverdyukova, 2017; Da Silva *et al.*, 2018;

Al Mohammadi *et al.*, 2020; Khannoon *et al.*, 2020). In contrast, the fusion of both dorsal laminae of the parietal in *A. brongersmianus* occurs shortly before hatching, as evidenced by a fissure in the posteromedial region of the parietal in the hatchling (Fig. 2D). Likewise, other authors reported a mid-sagittal fontanelle or paired parietals in juvenile typhlopid snakes—*Anilios bicolor* and *Typhlops jamaicensis* (Shaw, 1802)—where left and right counterparts later co-ossify in a single parietal in adults (Evans, 1955; Palci *et al.*, 2016). Therefore, the closure of the skull roof is a delayed process in blind snakes with respect to what occurs in alethinophidians, and may take place during postnatal ontogeny in some species.

Intraspecific variation on the parietal condition of *Typhlops pusillus* Barbour, 1914 has been inferred, since it was variably reported as paired (List, 1966) or fused (Thomas, 1976). However, List (1966) probably based his observation on an immature specimen, and the paired parietal condition is a misinterpretation of this author. Thus, the few available records on discrepancies of the parietal condition for the same species are not sufficiently sustained to consider this as an intraspecifically variable character. In addition, total length of the individuals, which may be a good proxy of age and hence ontogenetic stage, is not always provided in osteological descriptions. Accordingly, data on size (as total length or snout-vent length) of specimens should be addressed, so that future studies can take this information into account and benefit from it.

The persistence of an embryonic trait such as the parietal fontanelle in juvenile (*Anilios bicolor*) or adult stages (e.g. *Namibiana* Hedges, Adalsteinsson & Branch, 2009 and *Myriopholis* Hedges, Adalsteinsson & Branch, 2009) of blind snake species (Palci *et al.*, 2016; Broadley & Wallach, 2007; Cundall & Irish, 2008; C.K., pers. obs.) may appear counterintuitive for fossorial organisms that are first-head burrowers (Herrel *et al.*, 2021), and has been posed as a non-adaptive ontogenetic constraint (Palci *et al.*, 2016). However, providing an adaptive explanation for every skull structure overlooks the idea that each ontogenetic stage is a fully functional unique organism. In this sense, the absence of a completely ossified braincase roof in early postnatal stages, juveniles or adults of some blind snake species indicates that this is not a prerequisite for burrowing. Furthermore, we hypothesize that a behavioural trade-off during postnatal ontogeny could exist, and those stages with incomplete ossification of the skull roof can either use tunnels and crevices of the nests of social insects or those elaborated by adult congeners, or they can even live in loose substrates.

OTIC REGION

Lira & Martins (2021) reported interspecific variation regarding the participation of the prootic and the parabasisphenoid in the formation of the trigeminal foramen in *Amerotyphlops reticulatus* (Linnaeus, 1758) and *A. brongersmianus*. These authors also claimed that this character does not vary intraspecifically within blind snakes, and might be relevant in terms of diagnostic characters for species. However, we observed postnatal ontogenetic variation in this character in *A. brongersmianus* (Fig. 3E, F). Interestingly, the configuration of the trigeminal foramen in the *A. reticulatus* specimen of Lira & Martins (2021) is the same as that observed herein in the subadult of *A. brongersmianus* (Fig. 3E). The ontogenetic variation of a character may hide the presence of interspecific variation or, on the contrary, show false interspecific variation. The latter may be the case of the specimen of *A. reticulatus* of Lira & Martins (2021), since the character may have not completed its ontogenetic trajectory. In consequence, the taxonomic value of the formation of the trigeminal foramen is challenged, at least for *Amerotyphlops* species.

In most squamates, the opisthotic and exoccipital fuse during embryonic development to form the otooccipital bone (Greer, 1985; Estes *et al.*, 1988; Maisano, 2001), although there are few records of unfused condition in hatchlings of lizards (Rieppel, 1992a, b, c), and of a suture between both elements in the neonates of *Lacerta agilis* Linnaeus, 1758 (Rieppel, 1994) and of xantusids (Maisano, 2002). In spite of this character being considered phylogenetically informative for squamates (Estes *et al.*, 1988; Evans, 2008), it has received little attention in ontogenetic studies of snakes. As such, the presence of a suture at an early postnatal stage was only explicitly reported by Rieppel & Zaher (2001) for the caenophidian snake *Acrochordus granulatus* (Schneider, 1799). Hence, we report here for the first time, evidence of the onset of embryonic fusion of the exoccipital and opisthotic in a blind snake, and persistence of the suture between these bones in the hatchling stage of *A. brongersmianus* is also indicative of delayed fusion of these bones during embryonic ontogeny in comparison to alethinophidians.

BASICRANIUM

Of the two elements that constitute the adult basicranium in snakes, the parabasisphenoid bone exhibits the most complex ontogenetic trajectory. This bone results from the fusion of the membranous parasphenoid and the chondral basisphenoid (De Beer, 1937; Bellairs & Kamal, 1981). The parasphenoid ossifies in the anterior region of the braincase

floor, between the anterior ramus of the trabeculae cranii, while the embryogenesis of the basisphenoid involves the perichondral/endochondral ossification of the trabeculae cranii and crista sellaris, as well as membrane bone outgrowths closely related with these chondrocranial structures (De Beer, 1937; Bellairs & Kamal, 1981; Haluska & Alberch, 1983; Rieppel, 1988).

The alethinophidian parabasisphenoid was traditionally characterized by the development of broad lateral wings corresponding to those ossifications lateral to the trabeculae, and labelled with different names in literature [e.g. lateral bony wing of the parasphenoid, lateral ascending wing of the sphenoid, among others (McDowell, 1967, 2008; Rieppel, 1979a, b, 1988)]. Furthermore, the posterolateral region of the parabasisphenoid bone forms a complex structure for the passage of vessels and nerves—the cerebral carotid artery and the palatine ramus of the facial (VII) nerve—which gained an intracranial course during the evolution of the snake braincase (McDowell, 2008). Some authors claimed that the parabasisphenoid wings were absent in blind snakes, and that this character differentiated them from alethinophidians (McDowell, 1967; Rieppel, 1979a, 1988; Rieppel & Zaher, 2000). These authors also related the absence of this structure with the lack of a closed Vidian canal, a structure largely highlighted as an alethinophidian feature (McDowell, 1967; Rieppel, 1979b; Rieppel & Zaher, 2000). Of note are the available ontogenetic series of *A. brongersmianus* showing a well-developed ossification laterally to the trabeculae, and a well-defined posterior region of the Vidian canal, which is floored during the ontogeny in the same fashion as observed in alethinophidians (Figs 3, 6). Moreover, the intracranial course of the Vidian canal of *A. brongersmianus* resembles that of other alethinophidians such as *Anilius scytale* (Linnaeus, 1758) or the caenophidian *Homoroselaps lacteus* (Linnaeus, 1758) (Rieppel, 1979b; A.S., pers. obs.). Hence, an ossification lateral to the trabecula and a closed Vidian canal as a passage for the palatine nerve and the cerebral carotid is not an exclusive character of alethinophidians, but seems to be a common feature of extant snakes.

CLOSURE OF THE BRAINCASE AND BURROWING

The descending processes of the frontal and parietal bones reach the parasphenoid rostrum and the parabasisphenoid wings in snakes, performing the lateral closure of the braincase, which represents an exclusive character of snakes among squamates (Bellairs & Underwood, 1951). A completely enclosed braincase, also reinforced by wide sutural contacts between bony elements, has been historically linked to fossoriality as a response to mechanical stress in head-first burrowers (Gans, 1974; Savitzky, 1983).

However, whereas most extant snakes exhibit a well-developed suture contact between the floor and lateral wall of the braincase, the highly fossorial blind snakes can display loose contact between braincase elements, including fissures filled with fibrous connective tissue (List, 1966; McDowell, 1967; Cundall & Irish, 2008; Palci *et al.*, 2016). Moreover, the braincase of other active burrowing squamatans such as amphisbaenians fails to fully enclose the endocranial cavity (Gans & Montero, 2008). As such, the relation between a walled and strongly reinforced braincase and burrowing habits does not seem to be straightforward.

Our ontogenetic study indicates that the braincase of the typhlopid *A. brongersmianus* undergoes gradual reinforcement during postnatal growth, exhibiting fissures or simple contacts between braincase elements in the juvenile and the subadult stages. This condition of early postnatal stages, as well as the paired parietals or poorly ossified skull roofs, was interpreted as 'maladaptive' or temporarily non-adaptive for burrowing blind snakes (Palci *et al.*, 2016). Recently, the first comparative survey about burrowing forces in adult blind snakes posited that typhlopid snakes are able to generate higher forces for a given body length compared to other blind snakes and burrowing alethinophidians (Herrel *et al.*, 2021). Considering this observation, and as mentioned above, we hypothesized about this apparent counterintuitive issue by proposing the existence of a behavioural trade-off along postnatal ontogeny. Young blind snakes may use formerly excavated tunnels such as those of insect nests, and probably increase their burrowing capabilities during postnatal advanced stages when skull ossification increases and bone contact is reinforced.

Interestingly, other skull traits traditionally considered crucial for burrowing in snakes have been recently challenged (Deufel, 2017). The shield-nosed cobra *Aspidelaps scutatus* (Smith, 1849) was described as being able to excavate and construct tunnels in loose substrates with a typical highly kinetic skull present in other surface-dwelling alethinophidians (Deufel, 2017). The apparent eco-morphological mismatch between non-solid/kinetic skulls of burrowing snakes can be interpreted as a case of 'organic nonoptimal constrained evolution' (Diogo, 2017). As such, it seems to be plausible that there are different morphologies and trade-offs in burrowing snakes that constitute different mechanisms for burrowing, a complex behaviour that repeatedly appeared in the evolutionary history of snakes.

GROWTH OF THE GNATHIC COMPLEX

Since the early works it has been highlighted that the gnathic complex of blind snakes strongly departs

from the rest of the squamates (Haas, 1930; Dunn & Tihen, 1944; Tihen, 1945; Evans, 1955). Shortening and simplification of bony elements, lack of teeth in typically toothed bones, and loss of elements of the suspensorium are the most remarkable transformations present in blind snakes (Cundall & Irish, 2008). Additionally, bones of the gnathic complex experience isometric or even negative allometric growth during postnatal ontogeny (Palci *et al.*, 2016; Scanferla, 2016). In this sense, *A. brongersmianus* displays a distinctive growth pattern of the bones of the gnathic complex (Fig. 8). The length of the quadrate shows a general growth of a negative allometric type, in accordance with the growth pattern described by Palci *et al.* (2016) for the typhlopid *Anilios bicolor*. In contrast, the pterygoid bone experiences remarkable longitudinal growth (Fig. 8) during postnatal ontogeny similar to that observed in macrostomous alethinophidian snakes (Fig. 8; Rossman, 1980; Scanferla, 2016). This is an unexpected trait for a non-macrostomous snake, since the pterygoid of macrostomous alethinophidians exhibits positive allometry, whereas most lizards and non-macrostomous snakes show isometric growth (Scanferla, 2016). Notably, the rod-like pterygoid in typhlopids serves as the insertion of the m. protractor pterygoidei, which almost entirely sheathes the bone (Haas, 1930; Iordansky, 1997). This muscle produces the forward displacement of the pterygoid and the consequent erection of the maxilla (Cundall & Rossman, 1993; Iordansky, 1997). As such, elongation of the pterygoid may be promoted by postnatal development of this muscle, whose insertion surface is relevant for muscle contraction during feeding.

Among the characters of the jaw complex of typhlopoids, the relative size reduction of the dentary also stands out (Strong *et al.*, 2021). Our results indicate that this morphology is the outcome of prenatal established proportions as well as postnatal isometric growth. This reduced dentary has consequences for mouth configuration, since the lower jaw is not in contact with the tip of the snout region when it is fully abducted. Therefore, a unique mouth configuration among squamates is set up. In accordance to the morphology of the gnathic complex, a highly specialized mechanism for the rapid ingestion and transport of large numbers of prey named 'single-axle maxillary raking' was described for typhlopoids (Iordansky, 1997; Kley, 2001; Strong *et al.*, 2021). The extremely short and toothless dentary of typhlopoids may constitute a functional prerequisite for this type of intraoral prey transport, since lower jaws simply act as passive scoops during feeding (Iordansky, 1997).

HETEROCHRONY, MINIATURIZATION AND THE EVOLUTION OF THE SKULL OF BLIND SNAKES

Heterochrony has been proposed as the most relevant developmental phenomenon producing morphological variation (De Beer, 1940; Gould, 1977; McKinney & McNamara, 1991). Therefore, heterochrony has been invoked to explain several osteological novelties of the snake bauplan and evolutionary trends in the group (Rieppel, 1988; Irish, 1989; Werneburg & Sánchez-Villagra, 2014; Da Silva *et al.*, 2018; Strong *et al.*, 2020). In particular, features of the highly modified skull of each blind snake clade have been explained through heterochrony, mostly assigned to paedomorphosis correlated with miniaturization (Rieppel, 1979a, 1988, 1996; Irish, 1989; Kley, 2006; Palci *et al.*, 2016; Strong *et al.*, 2019, 2020; Martins *et al.*, 2021). However, these hypotheses were largely based on adult morphology, which contributes with weak evidence to understanding heterochronic processes (Hanken, 1993). Moreover, the heterochronic change between species must be polarized by outgroup comparison in the context of a phylogenetic hypothesis, in order to identify the heterochronic process between ancestral and descendant ontogenies (Fink, 1982; Reilly *et al.*, 1997).

Our ontogenetic analysis of the skull of *A. brongersmianus* shows that development of some traits is clearly delayed regarding the developmental pattern seen in alethinophidians. This is the case of ossification of the parietals and the posterior region of the trabeculae cranii, fusion between opisthotic and exoccipital, and constitution of certain bony processes (e.g. postorbital and supratemporal processes of parietal). Ontogenetic trajectories of these characters do not have consequences on adult morphology, but their record allowed us to corroborate the previous hypothesis of peramorphosis through acceleration of ossification rates in alethinophidian skulls (Da Silva *et al.*, 2018). Furthermore, the ontogenetic data on the anguimorph lizards *La. borneensis* and *Varanus panoptes* Storr, 1980 (Werneburg *et al.*, 2015) suggests that the developmental rates of *A. brongersmianus* resemble those of lizards.

Among the cranial features, the skull roof of blind snakes has been pointed out repeatedly as a paedomorphic trait in the literature (Palci *et al.*, 2016; Da Silva *et al.*, 2018; Lira & Martins, 2021; Martins *et al.*, 2021). Although most species display an azygous parietal in adult forms, others exhibit paired bones in contact with one another, separated by a fissure of variable width, or even a large mid-sagittal fontanelle occupying the skull roof (Broadley & Wallach, 2007; Lira & Martins, 2021 and literature cited therein). Therefore, different configurations of the adult cranial roof in blind snakes can be obtained

either via prolongation or truncation of the ossification of the dorsal laminae of the parietals. Since there is no truncation of the skull roof development in *A. brongersmianus*, this trait cannot be termed as paedomorphic in this species, neither in Typhlopidae with an azygous parietal. However, poorly ossified skull roofs in adults of some blind snake taxa resemble the incompletely ossified skull roofs reported for postnatal stages in several lizard lineages (Maisano, 2001; Hernández-Jaimes *et al.*, 2012; Roscito & Rodriguez, 2012; Werneburg *et al.*, 2015; Skawiński *et al.*, 2021) and do indicate signs of paedomorphosis (Palci *et al.*, 2016; Da Silva *et al.*, 2018). Remarkably, these are forms belonging to the family Leptotyphlopidae, which is known for having a smaller overall size than typhlopids. Thus, it is worth asking if a relationship between adult skull roof morphology and mean adult body size can be established, or if a gradient in parietal ossification corresponding with decrease in adult body size exists along blind snake families?

The anteriorly oriented quadrate of blind snakes is a trait typically attributed to paedomorphosis (Caldwell, 2019; Strong *et al.*, 2020). Our observations of *A. brongersmianus* skull ontogeny showed that the quadrate has an almost horizontal orientation in embryos and remains the same during postnatal development. Limb-reduced lizards and non-macrostomous alethinophidian snakes have a vertically or slightly anteriorly oriented quadrate, and the lack of rotation along ontogeny was also reported for these groups (Montero *et al.*, 1999; Roscito & Rodriguez, 2012; Werneburg *et al.*, 2015; Scanferla, 2016). In contrast, the quadrate of macrostomous alethinophidians experiences a noteworthy counter-clockwise rotation during ontogeny (Bellairs & Kamal, 1981; Rieppel, 1988; Palci *et al.*, 2016; Scanferla, 2016). In this sense, the anteriorly oriented quadrate of adult blind snakes does not resemble the condition present in embryonic or juvenile stages of lizards and cannot be explained simply by truncation of the ancestral ontogenetic trajectory, as was previously noted by Rieppel (1988).

The most common effect of miniaturization on morphology is skeletal reduction and loss of bony elements (Hanken & Wake, 1993). Furthermore, miniaturization in tetrapods has been hypothesized as being caused mainly by paedomorphosis (Irish, 1989; Rieppel, 1996). However, in spite of miniaturized tetrapods showing a certain degree of paedomorphosis in skull morphology, there is a broad spectrum of effects from heterochronic development (Irish, 1989; Rieppel, 1996). In comparison to lizards and alethinophidian snakes, the skull of blind snakes exhibits strong reduction and loss of some cranial bones (e.g. supratemporal, jugal) and lack of teeth in different toothed bones (e.g. maxilla, dentary; Cundall

& Irish, 2008). These absences are not easily attributed to paedomorphosis but probably denote a more fundamental alteration of the processes underlying skeletal morphogenesis and bone differentiation (Hanken, 1993). Additionally, we observed some characters in the skull of *A. brongersmianus* that can be attributed to peramorphosis. The development of a crista circumfenestralis that completely closes the juxtastapedial recess represents a trait originated by an extension of the ancestral ontogenetic trend. Likewise, the allometric postnatal growth of the pterygoid bar observed in *A. brongersmianus*, resembling the growth pattern described for macrostomous alethinophidians (Scanferla, 2016) is another peramorphic trait of this blind snake species.

Finally, beyond the heterochronic traits discussed previously, there are further features present in the skull of blind snakes that can be linked to their basal position in the tree of extant snakes. The absence of typical alethinophidian bony structures, such as the medial frontal pillars and the ophidiosphenoid bone, can be better explained as plesiomorphies shared with stem snakes such as *Dinilysia patagonica* Smith-Woodward, 1901 (Zaher & Scanferla, 2012). Thus, the unique skull anatomy of blind snakes seems to represent a combination of plesiomorphic and highly autapomorphic features, shaped through a complex interplay of heterochronic development, miniaturization, functional demands of fossorial lifestyle and historical contingency.

CONCLUSION

The peculiarity of the skull anatomy of blind snakes appears to be the result of a combination of plesiomorphic traits shared with lizards and stem snakes, along with highly autapomorphic traits shaped via heterochronic processes and miniaturization. These traits have been influenced by functional constraints and selective pressures relative to a fossorial lifestyle. Our ontogenetic analysis of the skull of *A. brongersmianus* demonstrates that some features such as skull roof morphology, quadrate orientation or absence of some cranial bones cannot be assigned to paedomorphosis, while others can be attributed to peramorphic processes. The ontogenetic series studied herein evidenced that the development of some traits (closure of the skull roof, fusion of elements of otoccipital bone, ossification of the trabeculae cranii) is clearly delayed in comparison to the developmental patterns seen in alethinophidian snakes, and resemble those of anguimorph lizards. Furthermore, the morphology of the egg tooth, and the presence of lateral wings of the parabasisphenoid and the posterior region of the Vidian canal were described for the first time for the

group. Finally, we showed that different elements of the gnathic complex can have decoupled and even opposed growth patterns during postnatal ontogeny, and that the braincase of *A. brongersmianus* undergoes a gradual reinforcement during postnatal growth. Further information on the size and shape ontogenetic changes of the skull of members of the other clades of blind snakes is still needed. Additional studies to test the correlation between size and presence of paedomorphic cranial features, and whether there is any relevant phylogenetic relationship, are also necessary.

ACKNOWLEDGEMENTS

DATA AVAILABILITY

The data underlying this article will be shared on reasonable request to the corresponding author.

REFERENCES

Al Mohammadi AGA, **Khannoon ER**, **Evans SE. 2020.** The development of the osteocranium in the snake *Psammophis sibilans* (Serpentes: Lamprophiidae). *Journal of Anatomy* **236:** 117–131.

Anan'eva NB, **Orlov NL. 2013.** Egg teeth of squamate reptiles and their phylogenetic significance. *Biology Bulletin of the Russian Academy of Sciences* **40:** 600–605.

Bell JB, **Daza JD**, **Stanley EL**, **Laver RJ. 2021.** Unveiling the elusive: X-rays bring scolecophidian snakes out of the dark. *The Anatomical Record* **304:** 2110–2117.

Bellairs Ad'A, **Kamal AM. 1981.** The chondrocranium and the development of the skull in recent reptiles. In: Gans C, Parsons TS, eds. *Biology of the Reptilia, volume 11, morphology F*. London: Academic Press, 1–263.

Bellairs A'A, **Underwood G. 1951.** The origin of snakes. *Biological Reviews* **26:** 193–237.

Bhullar BAS. 2012. A phylogenetic approach to ontogeny and heterochrony in the fossil record: cranial evolution and development in anguimorphan lizards (Reptilia: Squamata). *Journal of Experimental Zoology B* **318:** 521–530.

Boback SM, **Dichter EK**, **Mistry HL. 2012.** A developmental staging series for the African house snake, *Boaedon* (*Lamprophis*) *fuliginosus*. *Zoology* **115:** 38–46.

Boughner JC, **Buchtova M**, **Fu K**, **Diewert V**, **Hallgrimsson B**, **Richman JM. 2007.** Embryonic development of *Python sebae* - I: staging criteria and macroscopic skeletal morphogenesis of the head and limbs. *Zoology* **110:** 212–230.

Broadley DG, **Wallach V. 2007.** A revision of the genus *Leptotyphlops* in northeastern Africa and southwestern Arabia (Serpentes: Leptotyphlopidae). *Zootaxa* **1408:** 1–78.

Burbrink FT, **Grazziotin FG**, **Pyron RA**, **Cundall D**, **Donnellan S**, **Irish F**, **Keogh JS**, **Kraus F**, **Murphy RW**, **Noonan B**, **Raxworthy CJ**, **Ruane S**, **Lemmon AR**, **Moriarty Lemmon E**, **Zaher H. 2020.** Interrogating genomic-scale data for Squamata (lizards, snakes, and amphisbaenians) shows no support for key traditional morphological relationships. *Systematic Biology* **69:** 502–520.

Caldwell MW. 2019. *The origin of snakes: morphology and the fossil record*. Boca Raton: Taylor & Francis.

Chretien J, **Wang-Claypool CY**, **Glaw F**, **Scherz MD. 2019.** The bizarre skull of *Xenotyphlops* sheds light on synapomorphies of Typhlopoidea. *Journal of Anatomy* **234:** 637–655.

Cundall D, **Greene HW. 2000.** Feeding in snakes. In: Schwenk K, ed. *Feeding: form, function and evolution in tetrapod vertebrates*. San Diego: Academic Press, 293–333.

Cundall D, **Irish F. 2008.** The snake skull. In: Gans C, Gaunt AS, Adler K, eds. *Biology of the Reptilia, volume 20, morphology H: the skull of Lepidosauria*. Ithaca: Society for the Study of Amphibians and Reptiles, 349–692.

Cundall D, **Rossman DA. 1993.** Cephalic anatomy of the rare Indonesian snake *Anomochilus weberi*. *Zoological Journal of the Linnean Society* **109:** 235–273.

De Beer GR. 1937. *The development of the vertebrate skull*. Oxford: Clarendon Press.

De Beer GR. 1940. *Embryos and ancestors*. Oxford: Oxford University Press.

De Beer GR. 1949. Caruncles and egg-teeth: some aspects of the concept of homology. *Proceedings of the Linnean Society of London* **161:** 218–224.

Da Silva FO, **Fabre A-C**, **Savriama Y**, **Ollonen J**, **Mahlow K**, **Herrel A**, **Müller J**, **Di-Poï N. 2018.** The ecological origins of snakes as revealed by skull evolution. *Nature Communications* **9:** 376.

Dehling JM, **Hinkel HH**, **Ensikat H-J**, **Babilon K**, **Fischer E. 2018.** A new blind snake of the genus *Letheobia* (Serpentes: Typhlopidae) from Rwanda with redescriptions of *L. gracilis* (Sternfeld, 1910) and *L. graueri* (Sternfeld, 1912) and the introduction of a non-invasive preparation procedure for scanning electron microscopy in zoology. *Zootaxa* **4378:** 480–490.

Deufel A. 2017. Burrowing with a kinetic snout in a snake (Elapidae: Aspidelaps scutatus). *Journal of Morphology* **278:** 1706–1715.

Diogo R. 2017. Etho-eco-morphological mismatches, an overlooked phenomenon in ecology, evolution and evo-devo that supports ONCE (organic nonoptimal constrained evolution) and the key evolutionary role of organismal behavior. *Frontiers in Ecology and Evolution* **5:** 3.

Dunn ER, **Tihen JA. 1944.** The skeletal anatomy of *Liotyphlops albirostris*. *Journal of Morphology* **74:** 287–295.

Estes R, **de Queiroz K**, **Gauthier J. 1988.** Phylogenetic relationships within Squamata. In: Estes R, Pregill G, eds. *Phylogenetic relationships of the lizard families*. Stanford: Stanford University Press, 119–281.

Evans HE. 1955. The osteology of a worm snake, *Typhlops jamaicensis* (Shaw). *The Anatomical Record* **122:** 381–396.

Evans SE. 2008. The skull of lizards and tuatara. In: Gans C, Gaunt AS, Adler K, eds. *Biology of the Reptilia, volume 20. morphology H: the skull of Lepidosauria*. Salt Lake City: Society for the Study of Amphibians and Reptiles, 1–347.

Fink WL. 1982. The conceptual relationship between ontogeny and phylogeny. *Paleobiology* **8:** 254–264.

Fioroni P. 1962. Der Eizahn und die Eischwiele der Reptilien. Eine zusammenfassende Darstellung. *Acta Anatomica* **49:** 328–366.

Fons JM, **Gaete M**, **Zahradnicek O**, **Landova M**, **Bandali H**, **Khannoon ER**, **Richman JM**, **Buchtova M**, **Tucker AS. 2019.** Getting out of an egg: merging of tooth germs to create an egg tooth in the snake. *Developmental Dynamics* **249:** 199–208.

Gans C. 1974. *Biomechanics: an approach to vertebrate biology*. Philadelphia: J.B. Lippincott Company.

Gans C, **Montero R. 2008.** An atlas of amphisbaenian skull anatomy. In: Gans C, Gaunt AS, Adler K, eds. *Biology of the Reptilia, volume 21, morphology I: the skull and appendicular locomotor apparatus of Lepidosauria*. Ithaca: Society for the Study of Amphibians and Reptiles, 621–738.

Gould SJ. 1977. *Ontogeny and phylogeny*. Cambridge: Harvard University Press.

Greer AE. 1985. The relationships of the lizard genera *Anelytropsis* and *Dibamus*. *Journal of Herpetology* **19:** 116–156.

Haas G. 1930. Uber das Kopfskelett und die Kaumuskulatur der Typhlopiden und Glauconiiden. *Zoologische Jahrbücher Abteilung für Anatomie und Ontogenie der Tiere* **52:** 1–94.

Haluska F, **Alberch P. 1983.** The cranial development of *Elaphe obsoleta* (Ophidia, Colubridae). *Journal of Morphology* **178:** 37–55.

Hanken J. 1993. Adaptation of bone growth to miniaturization of body size. In: Hall BK, ed. *Bone, volume 7: bone growth - B*. Boca Raton: CRC Press, 79–104.

Hanken J, **Wake DB. 1993.** Miniaturization of body size: organismal consequences and evolutionary significance. *Annual Review of Ecology, Evolution, and Systematics* **24:** 501–519.

Hermyt M, **Janiszewska K**, **Rupik W. 2020a.** Squamate egg tooth development revisited using three-dimensional reconstructions of brown anole (*Anolis sagrei*, Squamata, Dactyloidae) dentition. *Journal of Anatomy* **236:** 1004–1020.

Hermyt M, **Kaczmarek P**, **Kowalska M**, **Ruplik W. 2017.** Development of the egg tooth - The tool facilitating hatching of squamates: lessons from the grass snake *Natrix natrix*. *Zoologischer Anzeiger* **266:** 61–70.

Hermyt M, **Metscher B**, **Rupik W. 2020b.** Do all geckos hatch in the same way? Histological and 3D studies of egg tooth morphogenesis in the geckos *Eublepharis macularius* Blyth 1854 and *Lepidodactylus lugubris* Dumeril & Bibron 1836. *Journal of Morphology* **281:** 1313–1327.

Hernández-Jaimes C, **Jerez A**, **Ramírez-Pinilla MP. 2012.** Embryonic development of the skull of the Andean lizard *Ptychoglossus bicolor* (Squamata, Gymnophthalmidae). *Journal of Anatomy* **221:** 285–302.

Herrel A, **Lowie A**, **Miralles A**, **Gaucher P**, **Kley NJ**, **Measey J**, **Tolley KA. 2021.** Burrowing in blindsnakes: a preliminary analysis of burrowing forces and consequences for the evolution of morphology. *Anatomical Record* **304:** 2292–2302.

Iordansky NN. 1997. Jaw apparatus and feeding mechanics of *Typhlops* (Ophidia: Typhlopidae): a reconsideration. *Russian Journal of Herpetology* **4:** 120–127.

Irish FJ. 1989. The role of heterochrony in the origin of a novel bauplan: evolution of the ophidian skull. *Geobios, Mémoire Special* **12:** 227–233.

Jackson K. 2002. Post-ovipositional development of the monocled cobra, *Naja kaouthia* (Serpentes: Elapidae). *Zoology* **105:** 203–214.

Khannoon ER, **Evans SE. 2015.** The development of the skull of the Egyptian cobra *Naja h. haje* (Squamata: Serpentes: Elapidae). *PLoS One* **10:** e0122185.

Khannoon ER, **Ollonen J**, **Di-Poï N. 2020.** Embryonic development of skull bones in the Sahara horned viper (*Cerastes cerastes*), with new insights into structures related to the basicranium and braincase roof. *Journal of Anatomy* **237:** 1–19.

Kley NJ. 2001. Prey transport mechanisms in blindsnakes and the evolution of unilateral feeding systems in snakes. *American Zoologist* **41:** 1321–1337.

Kley NJ. 2006. Morphology of the lower jaw and suspensorium in the Texas blindsnake, *Leptotyphlops dulcis* (Scolecophidia: Leptotyphlopidae). *Journal of Morphology* **267:** 494–515.

Koch C, **Martins A**, **Schweiger S. 2019.** A century of waiting: description of a new *Epictia* Gray, 1845 (Serpentes: Leptotyphlopidae) based on specimens housed for more than 100 years in the collection of the Natural History Museum Vienna (NMW). *PeerJ* **7:** e7411.

Koch C, **Santa Cruz R**, **Cárdenas H. 2016.** Two new endemic species of *Epictia* Gray, 1845 (Serpentes: Leptotyphlopidae) from northern Peru. *Zootaxa* **4150:** 101–122.

Koch C, **Venegas PJ**, **Böhme W. 2015.** Three new endemic species of *Epictia* Gray, 1845 (Serpentes: Leptotyphlopidae) from the dry forest of northwestern Peru. *Zootaxa* **3964:** 228–244.

Kraus F. 2017. New species of blindsnakes (Squamata: Gerrhopilidae) from the offshore islands of Papua New Guinea. *Zootaxa* **4299:** 75–94.

Lira I, **Martins A. 2021.** Digging into blindsnakes' morphology: description of the skull, lower jaw, and cervical vertebrae of two *Amerotyphlops* (Hedges *et al.*, 2014) (Serpentes, Typhlopidae) with comments on the typhlopoidean skull morphological diversity. *The Anatomical Record* **304:** 2198–2214.

List JC. 1966. Comparative osteology of the snake families Typhlopidae and Leptotyphlopidae. *Illinois Biology Monographs* **36:** 1–112.

Maisano JA. 2001. A survey of state of ossification in neonatal squamates. *Herpetological Monographs* **15:** 135–157.

Maisano JA. 2002. Postnatal skeletal ontogeny in five xantusiids (Squamata: Scleroglossa). *Journal of Morphology* **254:** 1–38.

Martins A, **Koch C**, **Joshi M**, **Pinto R**, **Machado A**, **Lopes R**, **Passos P. 2021.** Evolutionary treasures hidden in the West Indies: comparative osteology and visceral morphology reveals intricate miniaturization in the insular genera *Mitophis* Hedges, Adalsteinsson & Branch, 2009 and *Tetracheilostoma* Jan, 1861 (Leptotyphlopidae: Epictinae: Tetracheilostomina). *The Anatomical Record* **304:** 2118–2148.

Martins A, **Koch C**, **Pinto R**, **Folly M**, **Fouquet A**, **Passos P. 2019.** From the inside out: discovery of a new genus of threadsnakes based on anatomical and molecular data, with discussion of the leptotyphlopid hemipenial morphology. *Journal of Zoological Systematics and Evolutionary Research* **57:** 840–863.

McDiarmid RW, **Campbell JA**, **Touré T. 1999.** *Snake species of the world. A taxonomic and geographic reference*, *Vol. 1*. Washington: The Herpetologists' League.

McDowell SB. 1967. Osteology of the Typhlopidae and Leptotyphlopidae: a critical review. *Copeia* **1967:** 686–692.

McDowell SB. 2008. The skull of serpentes. In: Gans C, Gaunt AS, Adler K, eds. *Biology of the Reptilia, volume 21, morphology I: the skull and appendicular locomotor apparatus of Lepidosauria*. Ithaca: Society for the Study of Amphibians and Reptiles, 467–620.

McKinney ML, **MacNamara K. 1991.** *Heterochrony: the evolution of ontogeny*. New York: Plenum Publishing Corporation.

Miralles A, **Marin J**, **Markus D**, **Herrel A**, **Hedges SB**, **Vidal N. 2018.** Molecular evidence for the paraphyly of Scolecophidia and its evolutionary implications. *Journal of Evolutionary Biology* **31:** 1782–1793.

Montero R, **Gans C**, **Lions ML. 1999.** Embryonic development of the skeleton of *Amphisbaena darwini heterozonata* (Squamata: Amphisbaenidae). *Journal of Morphology* **239:** 1–25.

Ollonen J, **Da Silva FO**, **Mahlow K**, **Di-Poï N. 2018.** Skull development, ossification pattern, and adult shape in the emerging lizard model organism *Pogona vitticeps*: a comparative analysis with other squamates. *Frontiers in Physiology* **9:** 278.

Palci A, **Caldwell MW. 2014.** The upper cretaceous snake *Dinilysia patagonica* Smith-Woodward, 1901, and the crista circumfenestralis of snakes. *Journal of Morphology* **275:** 1187–1200.

Palci A, **Lee MSY**, **Hutchinson MN. 2016.** Patterns of postnatal ontogeny of the skull and lower jaw of snakes as revealed by micro-CT scan data and three-dimensional geometric morphometrics. *Journal of Anatomy* **229:** 723–754.

Polachowski KM, **Werneburg I. 2013.** Late embryos and bony skull development in *Bothropoides jararaca* (Serpentes, Viperidae). *Zoology* **116:** 36–63.

R Core Team. **2020.** *R: a language and environment for statistical computing*. Vienna: R Foundation for Statistical Computing. Available at: https://www.R-project.org/

Reilly SM. 1997. An integrative approach to heterochrony: the distinction between interspecific and intraspecific phenomena. *Biological Journal of the Linnean Society* **60:** 119–143.

Rieppel O. 1979a. The braincase of *Typhlops* and *Leptotyphlops* (Reptilia: Serpentes). *Zoological Journal of the Linnean Society* **65:** 161–176.

Rieppel O. 1979b. The evolution of the basicranium in the Henophidia (Reptilia: Serpentes). *Zoological Journal of the Linnean Society* **66:** 411–431.

Rieppel O. 1988. A review of the origin of snakes. In: Hecht MK, Wallace B, Prance GT, eds. *Evolutionary biology*, *Vol. 22*. New York: Plenum Press, 37–130.

Rieppel O. 1992a. Studies on skeleton formation in reptiles. III. Patterns of ossification in the skeleton of *Lacerta vivipara* Jacquin (Reptilia, Squamata). *Fieldiana (Zoology)* **68:** 1–25.

Rieppel O. 1992b. Studies on skeleton formation in reptiles. I. The postembryonic development of the skeleton in *Cyrtodactylus pubisulcus* (Reptilia: Gekkonidae). *Journal of the Zoological Society of London* **227:** 87–100.

Rieppel O. 1992c. The skeleton of a juvenile *Lanthanotus* (Varanoidea). *Amphibia-Reptilia* **13:** 27–34.

Rieppel O. 1994. Studies in skeleton formation in reptiles. Patterns of ossification in the skeleton of *Lacerta agilis exigua* Eichwald (Reptilia, Squamata). *Journal of Herpetology* **28:** 145–153.

Rieppel O. 1996. Miniaturization in tetrapods: consequences for skull morphology. In: Miller PJ, ed. *Miniature vertebrates: the implications of small body size, vol. 69. Symposia of the Zoological Society of London*. Oxford: Clarendon Press, 47–61.

Rieppel O, **Kley NJ**, **Maisano JA. 2009.** Morphology of the skull of the white-nosed blindsnake, *Liotyphlops albirostris* (Scolecophidia: Anomalepididae). *Journal of Morphology* **270:** 536–557.

Rieppel O, **Zaher H. 2000.** The braincases of mosasaurs and *Varanus*, and the relationships of snakes. *Zoological Journal of the Linnean Society* **129:** 489–514.

Rieppel O, **Zaher H. 2001.** The development of the skull in *Acrochordus granulatus* (Schneider) (Reptilia: Serpentes), with special consideration of the otico-occipital complex. *Journal of Morphology* **249:** 252–266.

Roscito JG, **Rodrigues MT. 2012.** Skeletal development in the fossorial gymnophthalmids *Calyptommatus sinebrachiatus* and *Nothobachia ablephara*. *Zoology* **115:** 289–301.

Rossman CE. 1980. Ontogenetic changes in skull proportions of the diamondback water snake, *Nerodia rhombifera*. *Herpetologica* **36:** 42–46.

Sandoval MT, **Ruiz García JA**, **Alvarez BB. 2020.** Intrauterine and post-ovipositional embryonic development of *Amerotyphlops brongersmianus* (Vanzolini, 1976) (Serpentes: Typhlopidae) from northeastern Argentina. *Journal of Morphology* **281:** 523–535.

Savitzky AH. 1983. Coadapted character complexes among snakes: fossoriality, piscivory, and durophagy. *American Zoologist* **23:** 397–409.

Scanferla A. 2016. Postnatal ontogeny and the evolution of macrostomy in snakes. *Royal Society Open Science* **3:** 160612.

Shea GM. 2015. A new species of *Anilios* (Scolecophidia: Typhlopidae) from Central Australia. *Zootaxa* **4033:** 103–116.

Sheverdyukova HV. 2017. Development of the osteocranium in *Natrix natrix* (Serpentes, Colubridae) embryogenesis I: development of cranial base and cranial vault. *Zoomorphology* **136:** 131–143.

Skawiński T, **Skórzewski G**, **Borczyk B. 2021.** Embryonic development and perinatal skeleton in a limbless, viviparous lizard, *Anguis fragilis* (Squamata: Anguimorpha). *PeerJ* **9:** e11621.

Smith MA, **Bellairs AD**, **Miles AEW. 1952.** Observations on the premaxillary dentition of snakes with special reference to the eggtooth. *Zoological Journal of the Linnean Society* **42:** 260–268.

Strong CRC, **Palci A**, **Caldwell MW. 2020.** Insights into skull evolution in fossorial snakes, as revealed by the cranial morphology of *Atractaspis irregularis* (Serpentes: Colubroidea). *Journal of Anatomy* **238:** 146–172.

Strong CRC, **Scherz MD**, **Caldwell MW. 2021.** Deconstructing the gestalt: new concepts and tests of homology, as exemplified by a re-conceptualization of 'microstomy' in squamates. *The Anatomical Record* **304:** 2303–2351.

Strong CRC, **Simões TR**, **Caldwell MW**, **Doschak MR. 2019.** Cranial ontogeny of *Thamnophis radix* (Serpentes: Colubroidea) with a re-evaluation of current paradigms of snake skull evolution. *Royal Society Open Science* **6:** 182228.

Thomas JPR. 1976. *Systematics of the Antillean blindsnakes of the genus* Typhlops *(Serpentes: Typhlopidae)*. Published D.

Phil. Thesis, Louisiana State University and Agricultural & Mechanical College.

Tihen JA. 1945. Notes on the osteology of typhlopid snakes. *Copeia* **1945:** 204–210.

Trauth SE. 1988. Egg-tooth development and morphology in the six-lined racerunner, *Cnemidophorus sexlineatus* (Sauria: Teiidae), using scanning electron microscopy. *Journal of the Arkansas Academy of Science* **42:** 84–85.

Underwood G, **Lee MSY. 2000.** The egg teeth of dibamids and their bearing on possible relationships with gekkotan lizards. *Amphibia-Reptilia* **21:** 507–511.

Vidal N, **Hedges SB. 2005.** The phylogeny of squamate reptiles (lizards, snakes, and amphisbaenians) inferred from nine nuclear protein-coding genes. *Comptes Rendus Biologies* **328:** 1000–1008.

Vidal N, **Hedges SB. 2009.** The molecular evolutionary tree of lizards, snakes, and amphisbaenians. *Comptes Rendus Biologies* **332:** 129–139.

Vidal N, **Marin J**, **Morini M**, **Donnellan S**, **Branch WR**, **Thomas R**, **Vences M**, **Wynn A**, **Cruaud C**, **Hedges SB. 2010.** Blindsnake evolutionary tree reveals long history on Gondwana. *Biology Letters* **6:** 558–561.

Vitt LJ, **Caldwell JP. 2009.** *Herpetology: an introductory biology of amphibians and reptiles*. Burlington: Academic Press.

Werneburg I, **Polachowski KM**, **Hutchinson MN. 2015.** Bony skull development in the Argus monitor (Squamata, Varanidae, *Varanus panoptes*) with comments on developmental timing and adult anatomy. *Zoology* **118:** 255–280.

Werneburg I, **Sánchez-Villagra MR. 2014.** Skeletal heterochrony is associated with the anatomical specializations of snakes among squamate reptiles. *Evolution* **69:** 254–263.

Zaher H, **Scanferla CA. 2012.** The skull of the upper Cretaceous snake *Dinilysia patagonica* Smith-Woodward, 1901, and its phylogenetic position revisited. *Zoological Journal of the Linnean Society* **164:** 194–238.

SUPPORTING INFORMATION

Additional Supporting Information may be found in the online version of this article at the publisher's web-site:

Table S1. Micro-CT scanning parameters for each specimen analysed.